EUROPEAN COMMISSION

European Research Area

MICADO

Model Uncertainty for the Mechanism of Dissolution of Spent Fuel in Nuclear Waste Repository

PROJECT REPORT

EUR 24597 EN

Interested in European research?

Research*eu is our monthly magazine keeping you in touch with main developments (results, programmes, events, etc.). It is available in English, French, German and Spanish. A free sample copy or free subscription can be obtained from:

European Commission
Directorate-General for Research
Communication Unit
B-1049 Brussels
Fax (32-2) 29-58220

E-mail: research-eu@ec.europa.eu
Internet: http://ec.europa.eu/research/research-eu

EUROPEAN COMMISSION

Directorate-General for Research
Directorate J – Energy (Euratom
Unit 2 – Fission

Contact: Christophe Davies

European Commission
Office CDMA 1/61
B-1049 Brussels

Tel. (32-2) 296 16 70
Fax (32-2) 295 49 91
E-mail: christophe.davies@ec.europa.eu

EUROPEAN COMMISSION

nuclear science and technology

MICADO

Model Uncertainty for the Mechanism of Dissolution of Spent Fuel in Nuclear Waste Repository

Authors
B. Grambow (SUBATECH),
J. Bruno, L. Duro, J. Merino, A. Tamayo (AMPHOS),
C. Martin, G. Pepin, S. Schumacher (ANDRA), O. Smidt (BELV),
C. Ferry, C. Jegou (CEA),
J. Quiñones, E. Iglesias, N. Rodriguez Villagra, J. M. Nieto (CIEMAT),
A. Martínez-Esparza (ENRESA), A. Loida, V. Metz, B. Kienzler (FZK·INE),
G. Bracke (GRS), D. Pellegrini, G. Mathieu, V. Wasselin-Trupin, C. Serres (IRSN),
D. Wegen (JRC-ITU), M. Jonsson (KTH), L. Johnson (NAGRA),
K. Lemmens (SCK.CEN), J. Liu (SSM), K. Spahiu (SKB), E. Ekeroth STUDSVIK),
I. Casas, J. de Pablo (UPC), C. Watson, P. Robinson, D. Hodgkinson (Quintessa)

Contract No.: FI6W-036366

Final report

Work performed as part of the European Atomic Energy Community's R&T programme on Nuclear Energy 2002-2006, Area: Management of Radioactive Waste

2010 Directorate-General for Research Euratom EUR 24597 EN

EUROPE DIRECT is a service to helpyou find answers to your questions about the European Union

Freephone number (*):
00 800 6 7 8 9 10 11
(*) Certain mobile telephone operators do not allow access to 00 800 numbers or these calls may be billed

LEGAL NOTICE

Neither the European Commission nor any person acting on behalf of the Commission is responsible for the use which might be made of the following information.

The views expressed in this publication are the sole responsibility of the author and do not necessarily reflect the views of the European Commission.

A great deal of additional information on the European Union is available on the Internet.
It can be accessed through the Europa server (http://europa.eu).

Cataloguing data can be found at the end of this publication.

Luxembourg: Office for Official Publications of the European Communities, 2010

ISBN 978-92-79-17652-4
doi 10.2777/25846

© European Communities, 2010
Reproduction is authorised provided the source is acknowledged.

TABLE OF CONTENT

COORDINATION VI

EC PROJECT OFFICER VI

PROJECT WEB SITE VI

1 INTRODUCTION 1

1.1 MICADO APPROACH IN ASSESSING UNCERTAINTIES IN SPENT FUEL LONG-TERM PERFORMANCE MODELING 1

1.1.1 Summary description of project objectives: Central role of models in PA, central role of confidence in models 1

1.1.2 Contributing partners and discription of the project consortium 1

1.1.3 State of the art prior to the project: A generic fuel dissolution model 2

1.1.4 Work performed in the MICADO project and procedures used to assess data/model/conceptual uncertainties 3

2 DESCRIPTION OF MAIN PROJECT RESULTS: ASESSEMENT OF UNCERTAINTIES IN SPENT FUEL DISSOLUTION MODELS 6

2.1 UNCERTAINTIES IN BOUNDARY CONDITIONS 6

2.1.1 Common features in repository design concepts 6

2.1.2 Scenarios for exposure of spent fuel to groundwater 7

2.1.3 Evolution of disposal conditions 8

2.2 UNCERTAINTIES RELATED TO THE INITIAL STATE UNTIL FIRST THOUSANDS OF YEARS AFTER REPOSITORY CLOSURE 10

2.2.1 Main parameters and their uncertainties in initial state 10

2.2.2 Fuel modification in first thousands of years due to radioactive decay; container still assuring 100% confinement 14

2.3 UNCERTAINTIES FOR THE PERIOD OF THE FIRST HUNDREDS OF THOUSANDS OF YEARS IN HYDROGEN SATURATED REPOSITORY AFTER CONTAINER FAILURE : FUEL MATRIX DISSOLUTION 16

2.3.1 Experimental evidence on hydrogen effect and uncertainties in experimental rate values and U concentrations. 16

2.3.2 Uncertainties related to data interpretation: rate vs. solubility 22

2.3.3 Accessibility to grain boundaries 24

2.3.4 Uncertainties related to the radiolytical database (G-values etc.) 26
2.3.5 Uncertainties in models describing the H_2 effect 26
2.3.6 Uncertainties on fuel dissolution due to the effects of near field materials 29
2.3.7 Uncertainties relative to users of models 32
2.3.8 Proposition of a bounding case matrix dissolution rate in presence of hydrogen 32
2.4 PERIOD BEYOND HUNDREDS OF THOUSANDS OF YEARS : FUEL MATRIX DISSOLUTION UNDER REDUCING CONDITIONS WITHOUT HYDROGEN GAS 33
2.4.1 Evidence of UO_2 stability under reducing conditions from natural analogues 33
2.4.2 Uncertainties in radiolytic models close to or beyond dose threshold, including the effect of Fe^{2+} 34
2.4.3 Uncertainties in electrochemical models 35
2.4.4 Uncertainties on fuel dissolution due to the effects of near field materials 35
2.4.5 Proposition of a bounding case matrix dissolution rate under reducing conditions (or range) in the absence of hydrogen gas 35

3 CONSEQUENCES OF UNCERTAINTIES IN FUEL DISSOLUTION MODELING ON CONFIDENCE IN ASSESSMENT OF OVERALL REPOSITORY PERFORMANCE 37

3.1 SP1 37
3.2 SP2 38
3.3 CONCLUSIONS 41

4 FUTURE RESEARCH NEEDS 42

5 *REFERENCES* 45

List of partners

No.	Participant name	Participant short name	Country
1	Association pour la Recherche et le Développement des Méthodes et Processus industriels	ARMINES/ SUBATECH	FR
2	Agence nationale pour la Gestion des Déchets radioactifs	ANDRA	FR
3	Commissariat à l'Énergie atomique	CEA	FR
4	Centro de Investigaciones, Energéticas, Medioambientales y Tecnologicas	CIEMAT	ES
5	Empresa Nacional de Residuos Radiactivos, S.A	ENRESA	ES
6	AMPHOS XXI S.L. (former Enviros)	Amphos21	ES
7	Karlsruhe Institute of Technology, former Forschungszentrum Karlsruhe GmbH	KIT, FZK-INE	DE
8	Institut de Radioprotection et de Sûreté nucléaire	IRSN	FR
9	European Commission, Joint Research Centre, Institute for Transuranium	JRC-ITU	DE
10	Kungl Tekniska Högskolan	KTH	SE
11	Nationale Genossenschaft für die Lagerung radioaktiver Abfälle	NAGRA	CH
12	Studiecentrum voor Kernenergie – Centre d'Étude de l'Énergie nucléaire	SCK.CEN	BE
13	Svensk Kärnbränslehantering AB	SKB	SE
14	Swedish Nuclear Power Inspectorate	SKI	SE
15	Studsvik Nuclear AB	STUDSVIK	SE
16	Universitat Politecnica de Catalunya	UPC	ES
17	Gesellschaft für Anlagen- und Reaktorsicherheit mbH	GRS	DE
18	AVN	AVN	BE
19	Quintessa Limited	Quintessa	UK
20	Bel V	Bel V	BE

Coordination

Scientific: Bernd Grambow, Ecole des Mines de Nantes, SUBATECH, 4 rue Alfred Kastler, 44307 Nantes, France, grambow@subatech.in2p3.fr, ++33 2 51 85 84 70

Administrativ: Pauline Borgniet, ARMINES, Direction des Affaires Europeens, 60 boulevard Saint Michel ,75272 Paris Cedex 06, France, borgniet@ensmp.fr,

EC Project Officer

Mr Gaetano DI BARTOLO, European Commission, DG Research RTD.J.2: Office CDMA 1/58, B 1049 Bruxelles, Belgique, gaetano.di-bartolo@ec.europa.eu

Project Web site

http://micado.wikispaces.com/

1 Introduction

1.1 MICADO APPROACH IN ASSESSING UNCERTAINTIES IN SPENT FUEL LONG-TERM PERFORMANCE MODELING

1.1.1 Summary description of project objectives: Central role of models in PA, central role of confidence in models

Direct geological disposal of spent fuel from nuclear energy production is a waste management strategy of many European member states. Disposal safety must be ensured for hundreds of thousands to millions of years. If one wants to put the highly radioactive used nuclear fuel within a thick-walled metallic canister directly into a repository, corrosion of the canister will occur and access of deep groundwater will eventually take place. What happens if deep groundwater comes into contact with the fuel? Research has been ongoing for more than 25 years to create a large experimental data base to simulate the long-term performance of the fuel. Furthermore, there has been a substantial effort to develop descriptive and predictive modeling procedures. The evaluation of the long term performance of the spent fuel relies on the development of theoretical and sometimes semiempirical models which can be combined with more general safety assessment models allowing repository barrier performance predictions for overall repository performance assessment (PA). The coordinated action MICADO assesses the uncertainties in models describing the dissolution processes of spent nuclear fuel in a repository for geological time periods.

The objective is to find out whether international research has now provided sufficiently reliable models to assess the corrosion behaviour of spent fuel in groundwater and by this to contribute to answering the question whether the highly radioactive used fuel from nuclear reactors can be disposed of safely in a geological repository.

1.1.2 Contributing partners and discription of the project consortium

Coordinated by SUBATECH/ARMINES*, this international coordinated action joins the efforts of many European waste management agencies, technical support organisations for regulators, universities and research organisations. Participating organisations are CEA, ANDRA and IRSN from France, SCK.CEN and BEL-V form Belgium, KIT Karlsruhe (former FZK-INE), ITU and GRS from Germany, ENRESA, UPC, CIEMAT and AMPHOS21 from Spain, SKB, SSM, Studsvik and KTH from Sweden, NAGRA from Switzerland and Quintessa from the United Kingdom. Essentially most worldwide leading experts participate in the project, representing different approaches to the assessment of the performance of disposed spent fuel for very long times: based on electrochemical, geochemical and/or radiolytical modeling approaches. Based on inputs from such models and the associated experimental studies, simplified operational models for spent fuel dissolution are developed and used by waste management and regulating organisations for the safety assessments in more complex systems.

1.1.3 State of the art prior to the project: A generic fuel dissolution model

Depending on the heterogeneous distribution of radionuclides in the structure of spent fuel, their release to groundwater is classically described by the contribution of two fractions :

- A fast release of radionuclides which are not contained in the fuel matrix and which are released more or less instantaneously when the confinement (canister and fuel cladding) is breached and water enters the canister. This contribution is referred to as the *Instant Release Fraction (IRF).* The IRF tends to increase with increasing fuel burnup.
- A progressive and relatively slow release of the radionuclides which are embedded within the fuel matrix. This contribution is referred to as release by *Matrix dissolution*.

Performance assessment exercises demonstrate that in most of the scenarios, the long term radiation dose is dominated by the IRF, although it represents a small part of the total inventory. An IRF model has been developed within the European SFS project (5^{th} FWP) attributing low confinement properties to the various microstructures present within the fuel pellet: the fuel plenum, gap zone, fracture surfaces, the rim zone of high burnup spent fuel and grain boundaries. Due to helium generation, radiation, grain boundary-instability and long term diffusion effects, the radionuclide distribution in the spent fuel may evolve before water ingress in the canister and therefore the IRF may be different relative to the intermediate post-irradiation state.

Models for the dissolution of the spent nuclear fuel in groundwater focus on the effect of oxidants. Indeed, due to electrochemical reactions, under oxic conditions, fuel matrix dissolution is observed to be much faster than under reducing conditions. Locally oxidizing conditions may also occur even under initially anoxic geochemical conditions in deep groundwaters, due to the production of oxidants by the radiation field of the spent nuclear fuel. During the first few hundreds of years of disposal, a strong gamma radiation field is dominant but the spent fuel is not expected to be affected since there the metal container is expected to remain an effective barrier for far longer time. Even in the unexpected case of early container failure, presence of hydrogen from container corrosion will counteract radiolytic effects as has been show experimentally with fresh spent fuel. This oxidating effect of radiation will become lower with time since due to radioactive decay the effect of radiation decreases. In the long-term, essentially only alpha radiolysis is important. The irradiation of groundwater by alpha particles from the spent fuel leads to the dissociation of water molecules along the alpha track producing radiolytic reaction products. Part of these products are radical or molecular oxidants which can oxidise the fuel surface resulting in the formation of U(VI) as evidenced by XPS results. These U(VI)-species are subsequently released into solution as a function of the water chemistry, in particular as a function of carbonate concentration or they are fixed on the surface in form of secondary phases. Secondary uranium containing phases may incorporate other radionuclides. Evidence from experiments suggests that alpha radiation exhibits only a weak oxidizing effect that may lead to slow oxidative dissolution s if no reducing agents are present, but that this may be countered effectively by the presence of H_2 and Fe(II) species that would be present in the repository near field. At a sufficiently low dose (“dose threshold”) radiation seems to become unable to sustain oxidative dissolution. In the absence of radiolysis, under reducing conditions, U(IV) solubility controlled fuel matrix dissolution would dominate. Particularly low dissolution rates are observed in presence of hydrogen.

Such empirical observations, even if consistent and qualitatively logical, require a modeling foundation and framework given the nature of the problem of long-term safety assessment. As a result, understanding the interactions of a time-dependent alpha-radiation field with UO_2 and reducing agents naturally present in the near field is of importance, as testing and evaluating various detailed models may provide a more rigorous basis for rationalizing and explaining various experimental observations.

A generic spent fuel dissolution model, developed in the SFS project is illustrated in the figure 1.

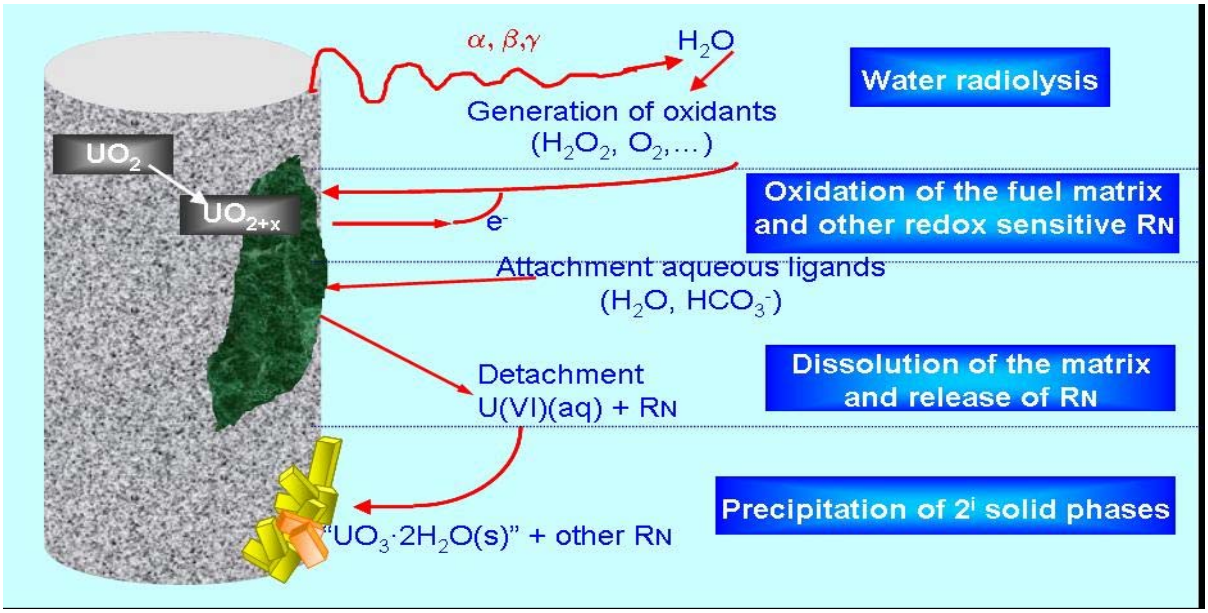


Figure 1: Elementary processes occurring in the fuel radiolytic dissolution

Basic steps for model development include (i) modelling of the generation of oxidants and reductants by a kinetic model of radiolysis, (ii) oxidation of spent fuel surface, (iii) reduction of the aqueous oxidants (only molecular species will be considered) and finally (iv) dissolution of spent fuel matrix and radionuclides release according to the uranium speciation and groundwater composition with or without consideration of electrochemical processes. G values and kinetic constants for the radiolytic model have been produced in the SFS project. Simplified models are also proposed, assuming for example that all produced oxidants will react with the fuel and that any fuel oxidation will lead also to fuel dissolution. More resent model development focus in particular on how to take into account the beneficial effect of hydrogen counteracting oxidative radiolytic dissolution. This includes radiolytic reactions of hydrogen in solution and at UO_2 surfaces.

1.1.4 Work performed in the MICADO project and procedures used to assess data/model/conceptual uncertainties

The project was addressing the following questions and missions:

1. Quantify model uncertainty in the effect of hydrogen on fuel dissolution. Considering the absence of realistic process models accounting for the stabilising effect of H_2, the question is how to avoid over-conservatism in ignoring this effect.

2. Quantify model uncertainty in the field of radiolysis and of electrochemistry.

3. Quantify model uncertainties in the assessment of grain boundary inventories and associated instant release fractions.

4. Quantify model uncertainty on the interface between spent fuel and the engineered barrier system (including corrosion products/metal fragment from the canister).

5. Quantify model uncertainty relating to the translation of knowledge assessed at laboratory scale to real scale of the spent fuel and according to industrial production of spent fuel in different countries.

6. Quantify model uncertainty in the extrapolation of short-term knowledge to very long time (geological times), taking into account different waste packages conditioning, disposal design used in different countries involved in the project.

7. How to avoid conflicts between model robustness and model realism in spent fuel PA and how to simplify models?

8. How to increase transparency in mechanistic hypothesis, model applications and model predictions?

The following procedures have been used to assess these questions.

Model authors and potential users (Waste management organizations, universities, research organizations, but not the TSO organizations) worked together in subproject SP1 with experimentalists and researchers with overall systems understanding in common expert groups within the different work packages after training in model use.

In a first group existing models were selected to apply to empirical data. Six models were exchanged between participants. This includes one IRF model from CEA and five matrix dissolution models. Detailed descriptions of the various models and documentation of the underlying assumptions have already been produced and are compiled and compared in a common document, showing how the known processes in the dissolution mechanism are represented in the model, and describing which processes are not considered in the model and which major uncertainties are encountered. Work was focused on fuel matrix dissolution models since the current state of knowledge on instant release fractions has already been well documented. Other project participants were trained so that they could work with these models without the presence of the authors of the models.

In another expert group, a common spent fuel/UO_2/MOX experimental database was selected, representing chemical data as well as radiolytical and electrochemical ones. Normalized questionnaires based on Excel worksheets were prepared and distributed to be filled by all the partners with their selected data. The data base covers the expected repository conditions both in the initial period (<50000 yr) characterised by high hydrogen/high radiation field environment and in the very long term (low hydrogen, low radiation field). Six instant release, 23 matrix alteration/dissolution, 7 radiolytical and 4 electrochemical experimental datasets were selected. In order to make the simulation exercise feasible, five experimental datasets have been selected as representative. In addition, a simple theoretical dataset has been developed to be applied by all modeling partners, which has been called Reference Case. In order to study the effect of hydrogen on the system, three different scenarios have been considered for the Reference Case, whose only difference is the initial hydrogen content.

The main goal of the next expert group was the comparison and uncertainty quantification of the source term models selected in the project. This model comparison was achieved by quantifying the uncertainties associated to the application of the models to the above mentioned experimental datasets selected. In particular, the models were applied to the reference case, to specific dissolution rate data as function of environmental variables, to radiolytic and electrochemical data and to the repository relevant part of the database. Deviations were documented.

The relevant information and approaches for assessing spent fuel behaviour for performance assessment were assessed. The uncertainty propagation to the overall safety analyses has been considered. Sensitivity and uncertainty analyses have been used to provide guidance on the significance of assumptions and uncertainties and to evaluate whether and to which degree uncertainties in predicted results are increased by this simplification.

An independent view was provided in subproject SP2 by an expert group composed of TSO organizations with a regulator point of view on the appreciation of the effects of documented model uncertainties on predictive uncertainties of the repository safety

1.1.4.1 Models whose uncertainties have been evaluated in the project

Only one instant release fraction model and 5 matrix dissolution models were compared. Only the CEA model for the IRF was discussed in MICADO. The original model was developed and documented in the EU SFS project [1] . A recent assessments by CEA of solid state radiation-enhanced diffusion and He build-up lead to an important reduction of uncertainties in the long-term evolution of the IRF values (Ferry et al. 2008).

The five matrix dissolution models evaluated are

Model 1 : The MAM model developed during the SFS project was represented by Amphos21, CIEMAT and ENRESA. It considers water radiolysis, geochemical solution and surface complexation reaction (kinetics). The model is calibrated with a large set of data on UO_2 dissolution as a function of pH, H_2O_2 and carbonates concentration and was successfully applied to data for UO_2 doped with alpha emitters as well as to spent fuel. The effect of hydrogen on spent fuel dissolution rates is described as a homogeneous effect in solution.

Model 2 was developed by KTH. It considers water radiolysis and diffusion of species and heterogeneous kinetics at the SF surface, making the hypothesis that only H_2O_2 production leads to spent fuel oxidation, and all oxidized spent fuel was conservatively considered as being dissolved. The justification of ignoring other radiolytic oxidants is that in systems dominated by alpha-radiolysis, the relative impact of H_2O_2 amounts to > 99.9 % of the total oxidation potential. Hydrogen effects are described by catalytic interaction with the epsilon phases.

Model 3 of SUBATECH considers also water radiolysis and diffusion of species. The radiolysis scheme is calculated with Maksima code and the radiolytic transport code Traramo is used to describe the effect of dose gradients at the fuel surface. In contrast to model 1, coupling between the water radiolysis model and the surface reactions of the spent fuel is not realized by surface complexation but by electrochemical reactions. The model has been calibrated against the same database as the MAM model. The effect of hydrogen is described by an effect of H_2 on the corrosion podential.

Model 4 of CEA is the French operational source term model. It only considers primary radiolytic species produced at the fuel surface and neglects conservatively reducing species and recombinisation of radicals. It assumes that 50% of the oxidizing species will be able to hit the fuel surface leading instantaneously to oxidation and dissolution of the fuel as U(VI). Secondary phase formation, reaction kinetics and the effect of hydrogen are neglected. It is a mass balance approach without fitting parameters.

Model 5 is another model of CEA. It consists of a complete radiolytic model and considers like model 3 dose gradients and diffusion of species. However, it can't be used for long-term calculations.

1.1.4.2 Limitation of project

The uncertainties in spent nuclear fuel dissolution models increase with burnup. At very high burnup fuel structures like the rim zone become increasingly important, but the density of experimental information decreases. IRF value uncertainties are assessed up to burnups of 75 MWd/kgU and matrix dissolution up to 60 MWd/kgU. Spent MOX fuel is excluded from the project since only very few experimental data are available, which do not yet allow uncertainty assessment.

Data for geochemical natural water environments in clay rock, salt and granite are considered, but the effects of certaines groundwater trace constituents like bromide, phosphate or fluoride

has not been assessed. Also hyperalkaline conditions were excluded from the assessment since only few data are available. Quantitative assessment is limited to room temperature data since groundwater access to the spent fuel in the thermal phase is excluded by the stability of the container, but TSO organizations studied the uncertainties related to early container failure and therefore processes that occur at higher temperatures.

.

1.1.4.3 A different perspective: Technical Safety Organisations

For many years AVN, GRS, SSM and IRSN, as technical safety organisations for regulators (TSOs), have developed performance assessment methods and integrated codes. Their participation in MICADO has provided an opportunity to share experiences and practices related to spent fuel modelling with research and waste management organisations. Within MICADO, the TSOs have not participated in the collection of data on spent fuel nor in the elaboration of the results arising from the detailed spent fuel dissolution models, but instead have discussed with representatives of SP1 the integrated outputs of such models and associated data sets (i.e. the results of the work performed by the research organizations within MICADO) on the basis of their own expertise on the long term safety of repositories. The objective of these discussions was to clearly understand the derivation of the complex models and data in order to convert them into simplified integrated models and associated data for long term performance assessment. These interactions between SP1 and SP2 were a mutual exchange of experience and technical views highlighting possible common understanding or identifying possible areas of disagreement. This analysis was completed by the quantification of the influence of different options in deriving an integrated source term for radionuclide release and migration by addressing the following questions :

- For which repository situation(s) is the spent fuel source term of high importance in controlling flux activity release out of the repository?
- In these situations, what is the impact of source term uncertainties on the released activity?
- Which parameters have an influence and at which scale (process level vs. integrated level)?
- Which radionuclides are sensitive to these uncertainties and for which repository situations?

To deal with these questions, the TSO organisations have defined characteristic long term evolution scenarios for the repository. IRSN, AVN, GRS and Quintessa jointly defined calculation cases. The TSOs and Quintessa have performed calculations with their own codes (the IRSN code has been developed to back up its technical appraisal of a radioactive waste repository). Interpretation of uncertainty propagation on the radionuclide release and migration has been performed jointly by the TSOs on the basis of the questions addressed above.

2 Description of main project results: Asessement of uncertainties in spent fuel dissolution models

2.1 UNCERTAINTIES IN BOUNDARY CONDITIONS

2.1.1 Common features in repository design concepts

The modelling of spent fuel (SF) dissolution relies on a definition of the conditions to which SF is exposed in the repository as well as on a definition of the properties of SF at the time that the canister is assumed to be breached and for the evolution over time as dissolution proceeds. A

basic requirement for application of spent fuel dissolution models and their evaluation is knowledge of the hydrogeochemical conditions to which the fuel will be exposed including possible changes over time and a definition of repository materials that interact with pore water. These conditions have been described in the deliverable D4.1 (Johnson et al. 2008) for repositories in crystalline rock, plastic clay (Boom Clay) and claystone (Opalinus Clay and Callovo-Oxfordian Clay).

Engineered barrier concepts for the disposal of spent nuclear fuel vary significantly, but have in common a canister that may contain from 4 to 12 fuel assemblies, depending on the design and mass of the assemblies. The canisters typically are constructed from steel or from copper with a cast iron insert. The mass of iron in a canister varies from 8 to ~20 t, depending on the design of the canister. The canisters are typically surrounded by an engineered barrier that may be made of bentonite (e.g. crystalline rock disposal concepts and Nagra's clay host rock concept) or cement-based material, in the case of the Belgian disposal concept. The materials selected for engineered barriers play an important role in establishing geochemical and mass transport conditions that influence the dissolution behaviour of spent fuel as discussed below.

2.1.2 Scenarios for exposure of spent fuel to groundwater

Different evolutionary paths can be envisioned for SF, depending on the thermal evolution, which is controlled by various design parameters (e.g. canister loading, canister separation, age of fuel at time of disposal), and the expectation of canister breaching within the early thermal period vs. a later period of near-ambient temperature. These aspects are discussed here to provide a rationale and foundation for modelling and experimental studies that address the relevant phenomena, based on some of the relevant assessments of the processes for different national safety studies.

The number of defective fuel rods at the time of waste emplacement is likely to be very small, likely < 1 in 5000. Zircaloy cladding will corrode at a maximum rate of about 10 nm/y (Johnson and McGinnes 2002), releasing activation products and producing hydrogen. There is a possibility that some or even most of the cladding may fail by creep rupture and hydrogen-induced cracking (HIC) within the first hundreds of years after canister emplacement. The role that the cladding will play in limiting water and solute transport in a canister is difficult to quantify. When cladding failures occur by creep rupture or HIC, penetrations are likely to be hairline cracks (Poinssot 2001) and once the internal gas pressure is released, the cladding will no longer be in a stressed state. As a result, cladding is likely to be a partial barrier to water movement until such time as extensive corrosion leads to its mechanical degradation. This is likely to take many thousands of years. However, this effect is not considered in many of the published PA exercises and, conservatively, immediate failure is assumed.

Three situations can be envisaged regarding the conditions to which SF might be exposed

1) Before the water comes into contact with the fuel assemblies inside the container (T > 100°C, decreasing to ambient rock temperatures, depending on the lifetime of the canisters). Changes may occur to the properties of the Zircaloy and fuel matrix due to solid-state processes. Even though such solid-state processes may occur very slowly, they may nonetheless be important if they change the microstructure of the SF (e.g. increase the surface area).

2) After relatively early canister breaching, (300y-1000 y); which is considered in some safety assessments for a small number of canisters. Factors considered include the probability that

3) Over the long term, i.e., after ~10,000 years (nominal lifetime for a steel canister) to >100,000 years (Cu canister minimum lifetime). For these time frames temperatures vary from 15-50°C, depending on ambient host rock temperatures and thermal conductivities

2.1.3 Evolution of disposal conditions

Despite significant differences in details of disposal canister designs, choices of engineered barrier materials around the canister and pore water chemistry; there are important features in common that have a dominant impact on spent fuel dissolution. In particular, these include:

- Reducing groundwater conditions, both in the host rock (deep clay or crystalline rock), where redox chemistry is dominated by Fe(II) minerals and the presence of sulphides, and in the engineered barrier system, where the corrosion products Fe(II) and H_2 are produced as a result of corrosion of iron or steel by pore water
- Diffusion-dominated conditions near the spent fuel, as a result of low hydraulic conductivity of the host rock and/or the engineered barrier. These restrictive mass transport conditions limit the transport of H_2 from the near field, leading to sustained high H_2 partial pressure in the near field

In most disposal concepts, the pH conditions are near neutral, but the ONDRAF concept involves the use of cement in the near field, which would lead to high pH (~12.5 to 13.5).

The relevant environmental parameters within breached SF containers have been summarised in D4.1 for repositories in crystalline and clay host rock for various EBS design concepts and sites. The objective is to describe the chemistry and mass transport conditions that would be relevant to the application of various models for SF dissolution.

The crystalline host rock case is based on the Forsmark site conditions, which cover a broad range of chemical conditions from saline to very dilute groundwaters. The redox conditions are expected to be reducing, as a result of the corrosion of the cast iron insert of the copper canister. Dominant redox species are expected to be Fe(II) and H_2, the latter being present at high concentration (~10MPa) as result of very slow transport through the bentonite and the high entry pressure for H_2. Mass transport conditions are considered to be diffusive as the long as the bentonite barrier properties are preserved.

Repositories in two claystone host rocks, Opalinus Clay (Switzerland) and Callovo-Oxfordian Clay (France), have also been considered. In this case the chemical conditions are similar for the two sites, with slightly saline porewater of near-neutral pH. Under all conditions, mass transport is considered to be diffusive and redox conditions within breached canisters would be dominated by Fe(II) from canister corrosion. The partial pressure of H_2 is expected to remain elevated (5 – 10 MPa) as long as steel materials in the near field continue to corrode, which is on the order of 100,000 years or more.

In the case of a SF repository at the Boom Clay site, the Belgian supercontainer concept incorporates cementitious material. Two porewaters have been defined, young concrete water (pH = 13.5) and evolved concrete water (pH = 12.5), which will possibly come into contact with SF after breaching of the containers. Because of the fairly low corrosion rate of the C-steel overpack at high pH and assuming a relatively fast diffusion of the species in the young concrete water away from the near field, the spent fuel would come into contact with evolved concrete water rather than young concrete water. Clogging of the pores of the concrete by precipitation of carbonates could, however, block the diffusion and keep the pH at the overpack high. This is likely to happen, but the process cannot yet be quantified sufficiently. So, because of remaining uncertainties on the corrosion rate of the C-steel overpack and on the time scale of the evolution from young to evolved concrete water, one can conservatively assume that spent fuel will come into contact with young cement water at the time of breaching of the overpack and containers. This choice is indeed conservative, because the preliminary test results suggest that UO_2 is less stable at pH 13.5. than at pH 12.5. Apart from the type of concrete porewater, there is still some uncertainty associated with the prevailing hydrogen partial pressures at the time of canister breaching, which is expected to be sustained in the region of 2.2 to 3.5 MPa for more than 100,000 years. In modelling studies, it was not possible in the MICADO project to consider models for such hyperalkaline conditions.

Some previous studies have assumed that hydrogen would rapidly diffuse away from the near field of SF repositories. More recent results indicate that high hydrogen partial pressures will exist for very long periods of time in repositories using Fe-based canister materials with bentonite and concrete barriers in both clay and granite host rocks. This suggests that spent fuel dissolution models should have the capability to estimate dissolution rates for both high and low hydrogen partial pressure (i.e. ~5 to 0.1 MPa) environments (the latter being relevant to time frames of ~100,000 years or more) as well as to cover the full feasible range of other groundwater chemical parameters.

2.2 UNCERTAINTIES RELATED TO THE INITIAL STATE UNTIL FIRST THOUSANDS OF YEARS AFTER REPOSITORY CLOSURE

This chapter describes properties of the fuel relevant to dissolution which are valid for initial situation of the disposed fuel. In the first thousands of years, container failure is not expected. Hence, uncertainties in radionuclide release are not addressed. But since it is a property of the fuel in its initial state, the radionuclide inventory fraction is described which would become instantaneously release one water access would occur (Instant release fraction).

2.2.1 Main parameters and their uncertainties in initial state

2.2.1.1 Burnup ranges

The fuel burnup varies locally along the length of the rod and the pellet radius. However the mean burnup of the spent fuel is a well known parameter, and all data such as RN inventories refer to the mean burnup.

The burnup range depends on the reactor type and the approach determined by the reactor operator, although national regulators may specify a maximum average burnup limit. Fuel assembly burnup values range from 30 $GWd.t^{-1}$ to about 75 $GWd.t^{-1}$, with typical values being in the 40-50 $GWd.t^{-1}$ range. Due to the lack of leaching data on high burnup fuels, uncertainties on IRF increase with burnup.

2.2.1.2 Surface area relevant to dissolution data

The reaction rate of the fuel matrix will depend critically on the surface area. Dissolution rates as a function of environmental variables as well as of radiolytic effects are all normalized to surface area. Uncertainties in surface area are very large, up to 5 orders of magnitude for a given constant specific geometric surface area (see figure 2). However, there exists no proportionality in the relationship between surface area and dissolution rate. It has even been observed that, while surface area increases upon long term leaching, dissolution rates actually decrease [2]. Surface area normalized dissolution rates of multi-grain fragments are faster than the corresponding rates for powders without grain boundaries [3]. A number of reasons and detailed mechanism may account for such behavior, but no clear understanding exists today: different accessibility of grain boundaries, effect of trace elements [2], different reactivity of different parts of the accessible surface due different chemical processes in grain boundaries (radiolysis, saturation) as opposed to external surfaces, limited distribution of anodic dissolution sites…..All these facts lead to a situation where the uncertainties in the specific surface area of relevance for leaching are much smaller than the above mentioned 5 orders of magnitudes. Considering that surface area uncertainties translate directly to probabilistic variations in PA calculations to scale up leaching data, the MICADO project was focussed only on dissolution relevant surface area uncertainties. Surface area increase without concomitant increase in dissolution rates is not considered.

The specific surface area is also a function of burn-up, in particular due to the increasing thickness of the highly porous high surface rim region. In the past years it was thought of that there might be an evolution of surface area with time by fracturing due to He bubbles. This effect has been studied in detail by CEA and it is today not anymore considered a risk since the pressure buildup will not be sufficiently high (this may be different for MOX but we only consider UOX here).

The specific surface area of the spent fuel relevant for leaching shows a dependency on several factors, i.e., particle size distribution, surface oxidation state, alteration process, precipitation of secondary phases, etc..

Geometric surface area and fracturing: The leaching relevant surface area of the fuel is increased by the degree of fracturing during reactor operation. The geometric surface area of a hypothetical non-fractured spent fuel pellet is 0.6 cm^2/g. However, after reactor operation, the fuel is fractured into a series of fragments of different size. The geometric surface area of spent fuel fragments is about **2.5 cm^2/g** if only large mm sized fragments are considered, but it is **6 cm^2/g** (data of Gray and Wilson [3] without correction for surface roughness) if fuel particles of <150 μm are considered. It is clear that fracture surfaces participate into the leaching process, but there does not yet exist an assessment as to whether the rates in fractures are similar to free external surfaces or not. Two processes reduce dissolution rates in fractures relative to external surfaces: due to the closeness of two adjacent surfaces, the dose rate in water filled fractures is higher but due to the small fracture aperture of < 1μm much less radiolysis products are produced, allowing for less radiation enhanced dissolution. This effect is further enhanced by precipitation of oxidized solid reaction products like schoepite. Both processes are related to mass transfer limitations in fractures. Indeed, Forsyth [4] explained the decrease of initial fractional dissolution rates values of 10^{-4}/yr to final rates after many years of $3 \cdot 10^{-7}$/yr for fuel segments (with attached cladding, keeping all fragments in place) by the observed formation of solid precipitates, blocking water access to fracture surfaces. However, no analyses exist as to whether this process remains active also under reducing H_2 saturated conditions where much less precipitates are expected to be formed. In the MICADO project it is therefore assumed that fracture surfaces remain accessible.

Surface roughness factor. It is possible to correlate the mean geometric surface of the particle size distribution (PSD) with the BET specific surface area. This ratio is labeled in the bibliography as roughness factor [1]. Figure 2 shows the mean roughness factor for a large data base of uranium oxide solid [2]. Indeed by comparing BET surface with geometric a surface roughness factor of 3.5 can be obtained for spent fuel and a value of 3 for UO_2. However, since spent fuel contains partly accessible grain boundaries, surface roughness estimates may be too high and, therefore, the **surface roughness factor of 3** for UO_2 will be used.

Grain boundary accessibility (this parameter is considered here only to justify upper bounds for surface area choices, for a more detailed discussion see chapter 2.3.3): Like for unirradiated UO_2, BET measurements on spent fuel grains (no grain boundaries) give similar specific surface areas, as PSD measurements, corrected with a surface roughness factor of 3 [3] (RC-PSD=roughness corrected PSD. However, for multi-grain fuel particles BET surface area is much larger than RC-PSD estimates. Gray and Wilson [3] estimated a surface area increase due to accessibility of grain boundaries of about a factor of 6. Measurements by BET tend to overestimate the accessible surface since not all gas accessible surface is also water accessible. The water accessible surface may increase with burnup. Larger water accessible grain boundary surface areas are calculated from Cs release data when compared to U release [3]. The higher values obtained from Cs release were explained by potential precipitation of U in grain boundaries. All this data seem to indicate that BET surfaces are not necessarily higher than surface areas calculated form leach data and need to be considered to assess upper bounds of surface area choices.

Forsyth [6] measured BET surface area of spent fuel fragments of 43 MWd/kgU (all size fractions included) as 72 $cm^2 \cdot g^{-1}$, other measured values for size fractions < 2000 μm were 59, 79, 88 and 120 cm^2/g and Stout and Leider(1998) reported a value of 59 cm^2/g. Gray and Wilson [3] measured the BET surface area of high burn-up ATM106 fuel particles of a size range between 0.5 and 150 μm as 120 cm^2/g and Rölin et al. [5] for a fuel of similar burn-up measured a surface area of 300 cm^2/g for a size fraction between 250 and 500 μm. These latter two values are too high since they concern not the whole spent fuel but only a small size fraction. This also means that the value of 120 cm^2/g of Forsyth [6] must be considered as an outlier and we obtain an average BET surface area of in-reactor fragmented spent fuel of 71±15 cm^2/g.

This BET value of 71 cm^2/g is probably much too high as this corresponds to decladded fuel, where all fragment surfaces are readily accessible. Forsyth [4] has shown that the accessibility

of fragment surfaces strongly decreases with time. Dissolution rates of individual fragments under oxidizing conditions were about 8-10 times larger than that of fuel segments of 2 cm length with cladding attached.

Fuel oxidation: The oxidation of spent fuel seems to increase the surface areas. Gray and Wilson [3] observed an increase in the ratio BET/roughness corrected PSD from 6 for unoxidized ATM106 fuel to a value of 20 for the same spent fuel, oxidized to a state of U_4O_{9+X}. This indicates that fuel oxidation increases the accessibility of grain boundaries. However, no effect on leaching rates was observed, hence, enhancement of surface area by oxidation is not taken into account in MICADO in the assessments of leaching relevant surface areas.

Leaching: The specific surface area of spent fuel grains (absence of grain boundaries) was observed to increase by a factor of 5 upon leaching, without concomitant effect on leaching rates [3]. Hence this effect is not included in MICADO.

Choice of surface area ranges: If we use the surface roughness factor of 3 together with the geometric surface area of 0.00025 m^2/g of irradiated fuel fragments or of 0.0006 m^2/g for <150 µm sized powder, one obtaines a minimum surface area between 0.00075 m^2/g and 0.0018 m^2/g. Arbitrarily a **minimum value of 0.001 m^2/g** has been choosen to account for the fact that large fragments underestimate and <150 µm particles overestimate surface areas. The measured average BET surface area of **0.0071 m^2/g** for fragmented fuel has been selected as maximum value. The average value is 0.004 m^2/g, which is close to the value which has been proposed and used in the MICADO project by ANDRA (gray shadowed area in Figure 2).

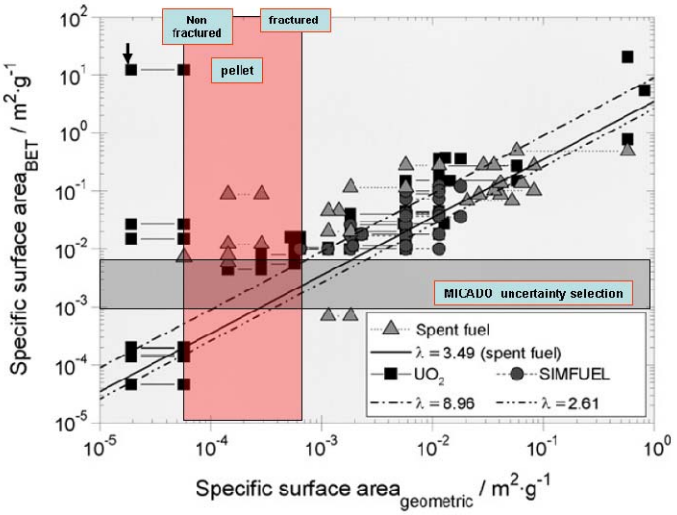


Figure 2 Roughness factor of uranium oxides [7]. The diagram includes bulk and powdered samples, an average surface roughness factor λ=3.5 (uncertainty 2.6 to 9) can be deduced for irradiated fuel

Uncertainties in surface area choices are critical for the translation between leach data for spent fuel and for unirradiated UO_2 or alpha doped materials. One may compare spent fuel and UO2 leach rates to assess whether the choice of specific spent fuel surface arease is reasonable. As an example, under oxic conditions, measured UO_2 dissolution rates are between 0.2 and 12 mg/m^2d. These rate values are used as such in the calibration of the MAM model. For comparison, typical fractional dissolution rates of spent fuel segments after some month to years are in the range between 10^{-6} to $2 \cdot 10^{-7}$/d. Using the suggested average specific surface area value of 0.004 m^2/g to convert fractional release rates to surface area normalized rates, one would obtain a surface area normalized spent fuel pellet dissolution rate under oxic conditions between 0.05 and 0.3 $mg \cdot m^{-2} \cdot d^{-1}$, clearly at or below the lower bound of the above mentioned rate data for unirradiated UO_2.under oxic conditions. In contrast, more realistic surface area normalized

rates between 0.2 and 1 $mg \cdot m^{-2} \cdot d^{-1}$ are obtained with the selected minimum surface area of 0.001 $m^2 \cdot g$, indicating that the minimum spent fuel pellet surface area might be more realistic thant the average value. Powdered samples of course have higher surface areas: With the the measured spent fuel powder surface area by BET of 0.03 m^2/g of Röling et al. [5], their leaching data under oxic conditions give a dissolution rate of 3 $mg/m^2/d$, very similar to those on UO_2, indicating that in this case BET data provide a good measure of the accessible surface area.

Furthermore, under reducing conditions spent fuel pellet dissolution rates are in the range of $10^{-9} \cdot d^{-1}$. leading with our average specific surface area to a surface area normalized dissolution rate of $3 \cdot 10^{-4}$ $mg.m^{-2} \cdot d^{-1}$ slightly lower than the rate values of 0.001 $mg \cdot m^{-2} \cdot d^{-1}$ measured on alpha doped UO_2 using the isotope dilution method (Olilla [8]). All this observations indicates that the selected specific surface area values conservatively overestimate the leaching relevant specific surface area of the fuel.

Important is not only the total surface area but the ratio of internal fracture surfaces to external surfaces, which we may define as surface fracturing factor. The surface fracturing factor will vary around a best estimate value of 15. Chemical and radiolytical fuel matrix dissolution rates cannot be scaled up directly with total surface area since fracture surfaces have different geometrical constraints than external surfaces. If we assume that the initial gap between fuel and cladding is about 85 µm as assumed in the MICADO reference case, we cannot assume the same water depth for fracture apertures since this will lead to water volumes in the fuel rod more than 6 times higher than the pellet volume. So we have to split the surface in different contributions, one coming from the outer surface (the geometric surface of the pellet multiplied only be the surface roughness factor) and the internal fracture surfaces, for which we might rather arbitrarily assign an irradiated solution depth of 1 µm. It shall be mentioned that the alpha dose rate in the fractures is about 8 times higher than the average one for a 30µm zone close to the outer surface since the surface dose in fractures is about 4 times higher than the average due to the closeness to the surface and the solution volume is irradiated by two adjacent surfaces. Mass transfer processes are much slower in fracture surfaces and cementation processes by reaction products will be much more important. It is known that the reaction rate of spent fuel under oxidizing conditions decreases over a period of up to 19 years from an initial rate of about 10^{-5}/day to a steady state long term value of about 10^{-7}/d [9]. It is likely that such decrease of reaction rate is caused by reduced access to fracture surfaces by formation of secondary reaction products such as schoepite (Forsyth 1997).

Using the above mentioned uncertainties in surface roughness, we may then distinguish the following uncertainties: the above mentionned uncertainty in total accessible specific surface area between 0.001 and 0.0072 $m^2 \cdot g^{-1}$ has to be subdivided for radiolysis calculations in two fractions, an external specific surface areas of (0.0002±0.0001) m^2/g^{-1} (including surface roughness) and an accessible internal specific fracture surface area between 0.0008 and 0.0069 $m^2 \cdot g^{-1}$.

2.2.1.3 Radionuclide inventory

The uncertainties associated with the inventories of radionuclides in spent fuel are generally considered to be rather small (< ~ 10 % for most fission products and < 20 % for most actinides) and can be calculated with validated isotope production/depletion codes. For ^{79}Se, the uncertainty remains significantly larger (perhaps a factor of 3) as a result of continuing uncertainties regarding its nuclear data. Uncertainties associated with the long-lived activation products ^{14}C and ^{36}Cl in fuel and structural materials arise principally from uncertainties in the concentrations of the precursor nuclides (principally ^{14}N and ^{35}Cl) in the unirradiated materials. Although the uncertainties in the concentrations of nuclide precursors may be significant, the radionuclide inventory calculations for performance assessment studies commonly use either realistic (measured) values or maximum permissible values of the precursors, thus ^{14}C and ^{36}Cl inventories are unlikely to be underestimated. (Reference D4.2)

2.2.1.4 IRF + uncertainty how to interprete leach data in terms of IRF

The Instant Release Fraction is a concept introduced in radionuclide source terms used for PA, where we distinguish the "rapid" release of radioactivity from the slow long-term release of radionuclides with the spent fuel matrix alteration.

A deterministic approach defines the IRF as the fraction of RN inventory located within the zone of the spent fuel rod with low confinement capacity on the long-term, i.e. after several thousands of years. IRF is the sum of two terms:

- The first one (IRF(t=0)) is the fraction of RN rapidly released by fresh irradiated fuels. Its values depend on the fuel burnup but also on the irradiation temperature (or linear power). Therefore the values proposed in the framework of MICADO refer only to PWR fuels operating under nominal conditions. They are based on the correlation between FGR data (fission gas release during irradiation) and leaching data available in literature. These data are rare for high burnup fuels and large uncertainties remain on this subject.

- The second one takes into account any evolution of the inventory availability prior to the arrival of water in the spent fuel rod (IRF(t))

By definition, IRF doesn't take into account any RN embedded in the SF grains (e.g. actinides). Indeed, these RN are released with the matrix dissolution.

In the concept of IRF, leach tests furnish the database of FP inventories located in the gap and voids of the SF rod and open grain boundaries at the end of irradiation, and the relation with the fuel mean burnup.

2.2.1.5 Solution volume in rod as function of BU related to life time of cladding and to free volume in corroded canister

The initial fuel sheet gap is about 85 μm but it closes with burnup. Forsyth [4] estimated the initial free volume in a fuel segment of 2 cm as 0.07 cm^3 and the value became reduced to 0.01 to 0.04 cm^3 after irradiation. The plenum volume of the fuel rods is initially about 19-24 cm^3 , and it is reduced after irradiation by 40%. Each fuel assembly of about 520-610 kg has a free volume of about 110-140 liters. In the concept of ANDRA there are 4 assemblies per fuel canister (1 for MOX).

2.2.2 Fuel modification in first thousands of years due to radioactive decay; container still assuring 100% confinement

2.2.2.1 Expected evolution of IRF values before container failure

IRF values, when water contacts the spent fuel surface (IRF(t)), depend on the evolution of the RN inventory location and microstructure due to α decays.

Experimental and modelling works on diffusion coefficients under disposal conditions show that the RN location will not evolve during the first thousands years of disposal.

As for the evolution of the pellet microstructure, it is governed by He fate in the spent fuel rod. A simplified approach indicates that He build-up would not have any consequences on the spent UO_2 fuel microstructure.

2.2.2.2 Uncertainties in models describing IRF=f(t)

The observations under 2.2.1 are consistent with He behaviour observed in implanted UO_2 and natural analogues. However the analogy with spent fuel is not complete (for example, the role of fission gas bubbles is not known) and large uncertainties remain concerning the SF mechanical properties.

IRF values take into account these uncertainties, by proposing best estimate, which corresponds to IRF(t=0), and pessimistic estimates, which include RN inventories located in the porosity of the restructured zones (rim). The fraction of RN inventories located in the rim porosity is not known, except for FG. The same fraction as derived from examinations for FG, are used for mobile RN, such as I and Cs.

2.2.2.3 Uncertainties in evolution of accessible surface area due to He generation (fractures?)

Micro-fracturing of the spent fuel pellet due to He generation will enhance the surface accessibility to water. According to the above paragraph, uncertainties remain on the evolution of the SF microstructure with He, and therefore on the SF surface area evolution during the first thousands years. In accordance with above discussion, a best estimate should be to take the SF surface area as measured on spent fuel fragments after irradiation.

The main question is: what should be the pessimistic value? Indeed, the increase of surface area with micro-cracking doesn't mean that it is the new surface area that should multiply the alteration rate as measured during leaching tests, where the solid/water ratio is relatively low, or derived from the matrix alteration model. Indeed, in dose calculations, we assume that the surface area is exposed to a water layer of at least 40 μm. This is not the case for the new surface areas, which may be exposed to water due to He effects.

2.3 UNCERTAINTIES FOR THE PERIOD OF THE FIRST HUNDREDS OF THOUSANDS OF YEARS IN HYDROGEN SATURATED REPOSITORY AFTER CONTAINER FAILURE : FUEL MATRIX DISSOLUTION

2.3.1 Experimental evidence on hydrogen effect and uncertainties in experimental rate values and U concentrations.

During the last decade, a number of tests with spent nuclear fuel or alpha doped UO_2(s) have been carried out in the presence of various amounts of dissolved hydrogen. In tests with relatively fresh spent fuel, the so-called hydrogen effect is observed for dissolved hydrogen concentrations higher than 0.8 mM, while much lower hydrogen concentrations are needed to in the case of α-doped material. By "hydrogen effect" it is usually meant a stronger effect of the dissolved hydrogen than the one accounted for by including hydrogen in the aqueous radiolytic scheme under the given experimental conditions. Lately evidence for the effect of metallic particles in causing a surface reduction of the uranium and inclusion of this process in the model have accounted for at least part of the hydrogen effect in the case of spent fuel. For α-doped UO_2, where ε-particles are absent, proposed or yet unknown processes at the solid solution interface may be responsible for the observations. The main lines of evidence for the hydrogen effect consist in the characteristics discussed shortly below, first for spent fuel tests and then for α-doped UO_2 tests.

Absence of molecular radiolytic oxidants. Spent fuel a few years after discharge from reactor has a high α-field (dose rates of the order of 1500 Gy/h) affecting a 30-40 μm water layer near the surface and a β-field with ranges up to 1 mm in water, while the γ-field affects the whole volume of the test solution.

Dissolved H_2 acts through a well known mechanism for radical rich (low LET) β- and γ-radiations in homogeneous solutions by scavenging the oxidizing OH-radical [10]:

$$H_2 + OH\cdot = H_2O + H\cdot \qquad k = 4\ 10^7\ L\ mol^{-1}\ s^{-1} \qquad (1)$$

This interaction converts the strongly oxidizing OH-radical into water and the reducing H-radical (atomic hydrogen), causing a general decrease of the concentrations of the oxidizing radical and molecular species. In any case, given that the molecular oxidizing species (H_2O_2 and O_2) are very reactive towards U(IV) in solution or in the solid phase or e.g. Fe(II) in solution, while the reducing molecular species (H_2) is considered inert at low temperatures, the radiolytic modeling of the whole system with excess H_2 predicts only a slower oxidation of the fuel matrix. Usually not all of the H_2O_2 produced near the spent fuel mainly by α-radiolysis reacts with its surface, a part diffuses away and the same holds for molecular oxygen. The continuous production of H_2O_2 by the strong α-field is expected to cause an increase of oxidant levels with time, in spite of its partial consumption in the bulk solution by the process described above. Direct measurements of O_2 and H_2O_2 in spent fuel leaching solutions in the presence of 0.8-43 mM dissolved H_2 [11,12,13,14,15] indicate levels below the detection limit (less than 10^{-7}-10^{-8} M). Another indication that these oxidant concentrations are extremely low comes from the low U concentrations (below $10^{-8.5}$ M), which indicate its presence in the tetravalent state. This state is stable only for extremely low O_2 fugacities [16]. It is generally accepted that H_2 does not react with H_2O_2 and O_2 at room temperature, thus

the extremely low concentrations of molecular radiolytic products observed under these tests are expected to be mainly due to surface-mediated processes.

Another indication on the importance of these surface processes comes from the recent tests carried out by adding 0.1 or 1 mM Br to the 5 M NaCl solutions in the presence of various amounts dissolved hydrogen [17,18]. Bromide is a known OH-radical scavenger, which reacts with the OH-radical about 250 times faster than molecular hydrogen [19] and impairs any beneficial effect of molecular hydrogen even under radical rich β, γ-radiations. Separate tests of 5 M NaCl solutions with added bromide in presence of H_2 showed extensive production of molecular radiolytic oxidants under external γ-radiation and oxidation of an added UO_2 pellet [18]. However, in tests with spent fuel in Br-containing solutions, where the intrinsic γ-radiation has apparently created the same conditions in the bulk solution, the measurements show absence of molecular oxidants in the autoclave, as well as low and decreasing concentrations of U or Pu [8]. In this case, since no beneficial effect of H_2 is expected in the case of homogeneous α-radiation [20], it follows that only surface mediated processes can be responsible for the consumption of the molecular oxidants produced near the fuel surface by α-radiation as well as the consumption of the oxidants produced in the bulk solution by intrinsic γ- or β-radiation.

All spent fuel tests discussed above were carried out in the presence of dissolved hydrogen concentrations higher than 0.8 mM. For the high radiation field of the spent fuel, the results of a test carried out with 0.08 mM dissolved hydrogen show that such low concentrations are not sufficient to counteract the oxidative dissolution of the fuel matrix [21]. In another series of tests, carried out in closed vessels with spent fuel and dissolved hydrogen concentrations of 0.056 mM or 0.24 mM, the presence of oxygen and hydrogen peroxide was verified through direct measurements [22]. On the other hand experimental data obtained with spent fuel in sealed glass ampoules in the presence of 10 mM $NaHCO_3$ show that after about one year a steady state is reached [23]. The concentrations of U and other matrix bound elements such as Cs and Sr are constant within experimental error for the ampoules opened after 1, 2 and 3 years reaction. These results could be modeled successfully [24] after introducing a surface reduction of U(VI) to U(IV) mediated by the ε-particles contained in spent fuel.

Decreasing concentrations of U and other redox-sensitive elements. The concentrations of U and other redox sensitive elements as Np, Pu, Tc etc. decrease during a few initial samplings, instead of increasing as expected under the strong radiation field. This decrease was observed in all spent fuel leaching tests in dilute carbonate containing solutions, including tests with MOX fuel which has a much stronger α-field [11,12,13,14,15,25,26,27,28] or in 5 M NaCl solutions [29,30]. Given the relatively low initial concentrations, this decrease is very probably due to the reduction by hydrogen of the oxidized forms released in solution at start by an initial pre-oxidized fuel

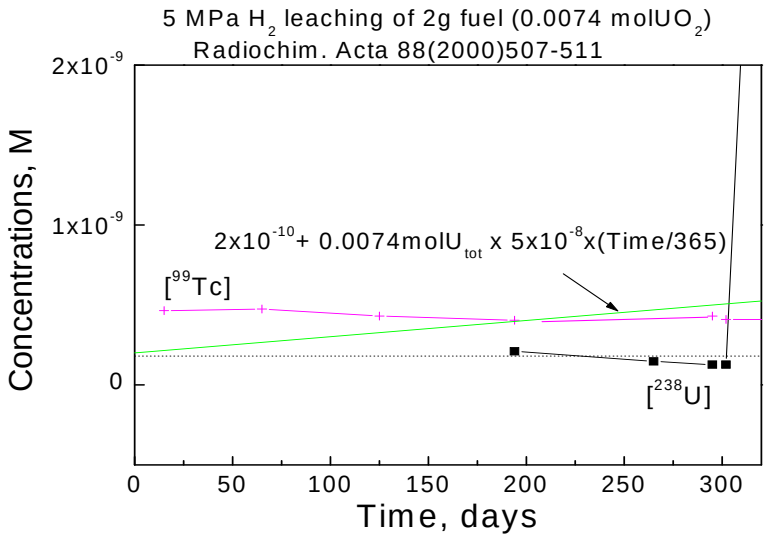


Fig. 3. Predicted U concentration (green line) for a fractional fuel dissolution rate of $5 \cdot 10^{-8}$/year, compared to measured U concentrations (filled squares). Tc is included because it is the only other nuclide in this test measured at such low concentrations. Similar graphs result for other experiments of this type.

surface layer. It is very probable that the same processes which cause the consumption of radiolytic molecular oxidants produce the surplus of active reductant causing the reduction of U(VI), Np(V) or Tc(VII). The concentrations of nearly all redox-sensitive nuclides from a pre-oxidized fuel layer decrease with time to values equivalent to the solubility of their reduced oxides. In all cases the concentrations of actinides, such as neptunium and plutonium, are two or more orders of magnitude lower than the uranium concentrations. The ratio between actinide and uranium is fairly close to that in the fuel [11,13,21], even though the solubilities of their tetravalent oxides are relatively similar. This indicates a possible co-precipitation of the pre-oxidized neptunium and plutonium with uranium, instead of the precipitation of separate dioxide phases, as well as a more convincing argument for the absence of any Pu(V) or Np(V) in solution. Similar behaviour has been noticed during a long term leaching experiment of the outer part of a high burn-up fuel pellet containing the rim zone or MOX fuel/5,6/.

Radolytic modeling studies of spent fuel dissolution, even when including a homogeneous reduction of U(VI) by hydrogen [31] or on the UO_2 surface[32], predict only a very slow increase of the U levels. In Fig. 1 an illustration of the experimental errors (around 20%, corresponds approximately to the size of symbols) in the determination of U at the relatively low concentrations is given. It is clear that the concentrations are low, but with today´s ICP-MS equipment fractions of a ppb U are almost routinely measured and especially an increasing trend in the analysis of several samples would certainly be observed (see Fig 3). The figure includes also a line representing the expected U concentrations for a fractional dissolution rate of $5 \cdot 10^{-8}$/year.

In the fuel leaching experiments in hydrogen-saturated solutions, it seems likely that the uranium and other redox-sensitive nuclides are deposited on the fuel surface, since very low levels of radionuclides were found in the vessel rinse [26]. More than 99% of the uranium was inferred to be precipitated on the surface of the spent fuel itself [27].
In the above discussion we consider relatively high concentrations of dissolved H_2 ($\geq$

0.8 mM, i.e. dilute solutions saturated with H_2 ≥1 atm), that is, several orders of magnitude higher than the concentrations of radiolytic oxidants or oxidized radionuclide species. This means that only a very small part of the total H_2 participates in these reactions, while the U precipitation rate seems to be strongly dependent on the fuel surface area and the temperature, but not much on the hydrogen surplus [13]. At room temperature the concentrations of U and other oxidized forms of radionuclides decrease to levels corresponding to the solubility of their tetravalent oxides after several hundred days [13,14,15]. The fact that they remain then constant (unless air contamination occurs) seems to rule out any simultaneous oxidative dissolution during their precipitation.
Finally, evidence for processes mediated by the fuel surface comes also from a co-dissolution tests of a spent fuel pellet with Fe(s) powder, started under Ar atmosphere and ended with 2.8 bar H_2 in Ar after 4 years corrosion [33, 34, 12]. Typical anoxic iron corrosion products as magnetite and green rust were observed on the iron indicating that the corrosion of iron in the same vessel as a spent fuel pellet occurred in absence of traces of oxygen. The analysis of iron after several hundred days shows negligible uranium sorption/precipitation, in spite of the decrease of the U concentrations during the test and the well known capacity of Fe(s) surfaces to cause rapid U(VI) reduction/precipitation [35,36]. This is in line with other observations that in presence of hydrogen very strong reducing conditions are created at the fuel surface.

Release rates of non-redox sensitive radionuclides and surface reduction. In the fuel case, the real material composition and the presence of non-redox-sensitive fission products makes it possible to judge the dissolution rate via their release rates. A systematic reduction by more than two orders of magnitude of the released fraction of ^{90}Sr or ^{137}Cs during successive time intervals was observed during more than one-year-long experiments under hydrogen atmosphere/11,12,13,21/. At longer leaching periods, the number of intervals where no releases of strontium or caesium could be measured increased. It is worth noting that after one year no more releases of Cs could be detected, even though more than 99% of the ^{137}Cs inventory was still inside the fuel matrix. The releases of ^{90}Sr decrease after much longer tests [28]; however, the total amount of ^{90}Sr released during the more than one year test is less than the amount contained in a monolayer of fuel sample [11,12]. This characteristic of the fuel leaching tests in presence of hydrogen with decreasing releases of non-redox sensitive radionuclides indicates for decreasing dissolution rates to very low values. A further confirmation of the decreasing Cs releases is obtained by the XPS analysis of the fuel surface before and after the one year test under 1 bar H_2 [13]. A clear Cs signal was observed in the initial fuel surface, while no Cs could be detected after the one year leaching test.

During the leaching phase under Ar after the tests of spent fuel leaching under 50 or 5 bar H_2 [21,28] the releases do not increase, in spite of the measured presence of oxygen in the autoclave [21] indicating for a reduced state of the surface. In the electrochemical test of a UO_2 electrode under 50 bar H_2 and γ- radiation [37,38], an irreversible reduction of the surface is reported. In addition, XPS-analysis of the fuel surface after long-term leaching under H_2 [13] and of an UO_2 pellet irradiated with an α-source under 1 bar H_2 also show a reduction of the UO_2 surface [39]. These data show that the number of oxidized sites in the UO_2 surface is practically zero and at the same time no increase of the U concentrations is observed.

The role of ε-particles in spent fuel and the mechanism of hydrogen action. Several recent studies have proposed mechanisms based on the catalytic effect of metallic ε-particles

(composed of the fission products Mo, Pd, Tc, Rh and Ru) on the H_2 activation at the fuel surface. The corrosion potential of SIMFUEL pellets decreased both with an increase in the number of ε-particles [40] and in dissolved hydrogen concentration [41] to values well below the UO_2(s) oxidation threshold, indicating complete inhibition of the fuel corrosion. Scanning electrochemical microscopy was used to verify that these effects can be attributed to the reversible decomposition of H_2 on metallic ε-particles [42].

Progress has been made also in modelling work at KTH resulting in the formulation of a steady-state model for fuel dissolution, using kinetic parameters determined in several dedicated studies / 34/. Studies of the catalytic effect of pure Pd particles on the reaction between H_2 and H_2O_2 show that the reaction is very fast, practically diffusion controlled and independent of the H_2 pressure in the range 1-40 bar [43]. Based on the reported decrease of the corrosion potential [41] and studies with Pd-doped UO_2 [44] the relevant parameters for the solid phase reduction of oxidized $U(VI)_{surf}$ mediated by hydrogen via ε-particles were estimated. The results of spent fuel dissolution modelling including the effect of Fe(II) ions in the decrease of the steady state H_2O_2 concentrations at the fuel surface and the fuel surface reduction process on ε-particles have been published recently [45].

The leaching behavior of ε-particles under Ar and Ar +10% H_2 shows that they are very active H_2-catalysts [46]. Further work is needed in the study of the role of metallic particles and the extent of galvanic coupling with UO_2 fuel matrix. Anyhow, it cannot be excluded that the radioactive actinide oxide surfaces also play a role in the observed surface mediated processes in the presence of dissolved H_2, as discussed in the following paragraph.

Experimental observations with α-doped UO_2.

After the first experiments with UO_2 doped with ^{233}U or ^{238}Pu, a few characteristics of these actinide oxide mixtures became clearer. First, a good quality of the pellets is required, since in some cases materials with low densities as compared to the theoretical UO_2 density give very high U releases [47]. Second, even with good quality pellets, the U releases at test start were proportional to the doping level, i.e. the amount of U released in solution from the pellet with 10 % ^{233}U was higher than this from the pellet with 1% ^{233}U, while releases from depleted UO_2 were lowest [48]. As it was shown later, these materials are quite sensitive to surface oxidation during storage [49,50], especially in the presence of a few layers of adsorbed water undergoing radiolysis.

Hydrogen influence on α-doped UO_2 dissolution: During the EU-project SFS, three tests with 10% ^{233}U doped UO_2 were carried out under various hydrogen concentrations [12]. The first was a batch test in carbonate-containing groundwaters flushed with Ar+6%H_2. Uranium concentrations decreased slightly with time for both 10% and 1% pellets. The pre-oxidation of the pellets [50] in the presence of adsorbed water while they were kept over the solution until the redox potentials became negative [12,48] may explain the higher start U concentrations (but lower than in Ar [12,48]) for the highest doped pellets. The second study was electrochemical [12] and the absence of carbonate in solution may be the cause of the quicker decrease of the U concentrations. The third test [12,51], carried out in an autoclave, started immediately after annealing. This may be part of an explanation for the extremely low U concentrations (10^{-11} M) measured. However, very low and constant U levels in the presence of α-radiolysis combined with the O_2 levels at the detection limit (10^{-8} M) suggest recombination reactions were occurring on the UO_2 surface. This is because reported measurements [20] on the production of H_2O_2 in H_2-saturated solutions during α-radiation (5 MeV He ions) show that in the presence of H_2 concentrations of 0.008 to 0.8 mM (0.01-1 bar H_2), practically the same amounts of H_2O_2 were measured under H_2 or Ar atmospheres. Recent

experiments carried out to study the influence of a larger excess (8 mM) of dissolved hydrogen on the oxidant production by α-radiolysis in ^{238}Pu solutions saturated with H_2 under 10 bar pressure indicate also no effect of dissolved H_2 as compared to Ar in the production of radiolytic O_2 [52]. After the conclusion of the autoclave test, the pellet was transferred in a vacuum drying vessel within minutes to an XPS instrument. No oxidation of the UO_2(s) surface could be detected by XPS.

In spite of these results, a clear observation of any hydrogen effect is complicated by the very limited effects of α-radiolysis even with pellets doped with 10 %^{233}U, where only a slight but measurable U increase is noted under Ar [48].

In the recent work by Muzeau et. al.[50], a UO_2 pellet with much higher doping level (385 MBq/g, corresponding to 50 y. old fuel) was also tested. In this case a very clear effect of α-radiolysis was observed under Ar atmosphere, with U concentrations increasing quickly with time in carbonate solutions. The same pellet was tested under 1 bar H_2 (3.3 bar Ar+30%H_2) and in this case the concentrations of U decrease slightly with time instead of increasing. Given the high rates of H_2O_2 production in this case and the fact a complete neutralization by H_2 in the bulk solution is not possible [20], only surface processes may be responsible for the neutralization of the produced H_2O_2, and for the observed decrease of the U levels with time. Another test with highly doped UO_2(s) (245 MBq/g) in powder form was carried out under the NF-PRO EU-project at SCK.CEN under 10 bar H_2. In spite of the high radiation field and surface area of the material, no increases were observed in the U concentrations in solution from day 90 to day 540, instead a slight decrease was observed [53].

Summary of the experimental uncertainties in hydrogen tests:

The general trends discussed above have been obtained under laboratory conditions with relatively pure systems. In most of the dilute solution tests the presence of ions as Ca, Mg or Si, known to decrease dissolution rates [53,54,55,56], has been avoided in the start solutions. Bicarbonate on the other hand has always been present (in the 2-10 mM range), in order to extract any oxidized U in solution. The role of potential precipitates in blocking the beneficial effect of ε-particles as well as the effect of catalyst poisons need still to be investigated.

Experimental data on alpha radiolysis of solutions containing relatively low concentrations of chloride ions (which also are expected to scavenge OH-radicals, though much less than bromide) and corresponding bromide concentrations, both in the presence and absence of dissolved H_2 need to be carried out. The higher reducing properties of Br^- are mainly expected to cause a decrease of the yield of hydrogen peroxide formed by α- radiolysis of dilute groundwaters, due to the consumption of part of the peroxide in reactions with bromide (e.g. iodide is used in the analysis of hydrogen peroxide due to its fast oxidation to I_2, which gives rise to the coloured I_3^- ion).

-Usually the dissolution rate in fuel tests has been determined by the increase of concentration of species released into solution. Uranium is the major component and easiest to measure, but under oxidizing conditions very soon saturation with some U(VI) phase is reached and the use of U to determine dissolution is not recommended. In tests under H_2, the formation of any secondary U(VI) phase can be excluded almost certainly and given the simple composition of test solutions, hardly any other phase than amorpous UO_2(s) is expected to form. Given the fact that the concentrations of U and other redox sensitive elements usually decrease in presence of H_2 (unless an extensive air contamination occurs) any rate determination based on U concentration evolution is difficult and at best “less

than" numbers can be reported. The same holds for FIAP and IRF values of non redox sensitive elements: due to the high surface area and small weight of the samples, these values are relatively high at start of the experiments, but very rapidly they decrease to values below detection limit. However, the XPS-analysis of a fuel sample leached for more than one year under 1 bar H_2 confirms depletion of Cs from the surface layer of the fuel which had a clear Cs peak before leaching [13].

Given the quasi stationary conditions in the fuel canister, it is important to evaluate the maximum extent of potential fast oxidative dissolution of spent fuel,. In the case of a high flow rate of reducing groundwater in the repository it is necessary to estimate the forward non-oxidative dissolution rate for UO_2. E.g. at SKB´s PA model[57] an immediate dissolution of the amount of UO_2 needed to saturate the solution is assumed. But based on the procedure described in p. 108 of reference [58], an estimation of the time to dissolve a UO_2 sphere of radius 1 mm using as dissolution rate 3 μg/(m^2 day)[5] and a molar volume of 24.64 cm^3/mol results in more than 10 million years. This has to be compared with the instantaneous dissolution assumed in PA models. On the other hand it is not clear whether larger safety margins are obtained if this apparent overconservatism in the PA models is replaced by a more realistic representation: Even with an extremely unrealistic high water flow of 1 $L \cdot s^{-1}$ per ton of uranium and a specific surface area of 0.0036 $m^2 \cdot g^{-1}$, solubility limits of U(IV) are achieved rapidly and U release from the fuel is solubility and not rate controlled.

2.3.2 Uncertainties related to data interpretation: rate vs. solubility

Redox conditions in water media are defined by pairs of pH and pe values, where pe is calculated as the Eh redox potential divided by the Nernst constant (59,16 mV at 298K). Under reducing conditions, the value of (pH+pe) must be close to zero.

Under reducing conditions, expected to occur in all European repository projects, in particular in presence of hydrogen from container corrosion, the spent nuclear fuel matrix is constituted by uranium (IV) dioxide as the thermodynamically stable phase, in equilibrium with aqueous U(IV) species. Under these conditions, an equilibrium state will be reached where the solubility of the SF matrix will be defined and which will give the maximum concentrations of uranium to be reached. After reaching solubility equilibrium solution concentrations of uranium are expected to remain constant. Since Uranium release originates from fuel matrix dissolution a corresponding inventory fraction of actinides, fission and activation products contained in this dissolved fuel matrix will also become mobilized and hence U solubility may control the release fraction of other radionuclides if the solubility of these nuclides is sufficiently high for not allowing precipitation in own secondary host phases.

An uncertainty remains however, whether dynamic exchange of dissolution and precipitation continues at solubility equilibrium. If this is not the case U solubility may under these conditions control the release of other radionuclides from the fuel matrix. There are however isotopic U238/235 exchange data [8], indicating that the reaction could continue with rate values between $3 \cdot 10^{-18}$ and $6 \cdot 10^{-19}$ $m \cdot s^{-1}$.(this is about 0.6 to 2.8 $\mu g.m^{-2}day^{-1}$ for the UO_2 density of 10.96 g/cm³), even if solubility equilibrium is reached. In this case a rate term will be needed to describe long term release of radionuclides under U-solubility controlled conditions.

Another uncertainty in using UO_2 solubility as control for the release of other elements is the possibility of U sorption on other solids (e.g. corroded iron…) or the formation of secondary U(IV) solid phases thermodynamically more stable than Uranium. Coffinite formation was long

times considered as a latter phase, but its formation conditions are rather poorly known and formation rates are expected to be very slow.

In case redox conditions are less reducing or even oxidizing (situation expected in the Yucca Mountain repository project), uranium (IV) dioxide is not the thermodynamically stable phase, and it may be oxidized to solid phases with a large variety of U(IV)/U(VI) ratios. Aqueous species will as well be constituted by U(VI) species. Under these conditions the evolution of the solid phase composition will clearly lead to a non-equilibrium situation with a kinetic rather than a thermodynamic control.

For a long time it was thought that radiation may create redox fronts at the surface of the fuel, leading to locally oxidizing conditions and to U(VI) formation. Recent model exercises of the NF-PRO project have shown that in presence of hydrogen from container corrosion, such redox fronts will break down.

SOLUBILITY:

Thermodynamic control: equilibrium (concentrations remain constant as far as the conditions of equilibrium are not altered)

Affected by:

- minor and major water composition (complexing agents, pH, Eh,....)
- temperature and pressure
- cristallinity of the solid phase (reprecipitation, radiation effect,...)
- particle size (for very small particles)
- sorption
- colloid formation

RATE:

Kinetic control: non-equilibrium (concentration is a function of time)

Affected by:

- minor and major water composition (complexing agents, pH, Eh,....)
- temperature and pressure
- cristallinity of the solid phase (reprecipitation, radiation effect,...)
- particle size (for very small particles)
- sorption
- colloid formation

Based on the statements above, uncertainties related to data interpretation may arise due to:

- Very low uranium concentrations measured under anoxic/reducing conditions, often close or below quantification limits, which makes difficult (if possible!) to see whether or not there is evolution of data as a function of time.
- Experimental difficulties to obtain and maintain strict reducing conditions for relatively long periods of time. Besides, chemical species used to keep those reducing conditions might interfere in the dissolution reaction.
- Cristallinity of the solid phase and/or presence of different degrees of cristallinity in the same sample which result in different concentration levels.
- Presence of small particles fractions of higher and faster dissolution.
- Presence of oxidized surface phases of higher and faster dissolution.
- Presence of secondary solid phases.
- Presence of colloids.

• Definition of the redox potential threshold where transition from thermodynamic to kinetic control takes place.

• Coexistence of U(IV) solid phase with U(VI) soluble species at certain pH-pe pairs of values, resulting in ambiguities when determining aqueous species formation constants.

•

Difficulties and uncertainties also increase when deducing from the behaviour of Uranium (for which the solution controls solubility vs. rate are rather well understood) to the behaviour of other radionuclides contained in the fuel matrix.

• U release might be solubility controlled but dynamic exchange (forward/backward rate) continues leading to rate control of the given element

• Under conditions of solubility control for uranium concentrations there might be a slow mass transfer rate of uranium to sorption sites on other materials, leading to a concomitant release of radionuclides

2.3.3 Accessibility to grain boundaries

Two different processes can potentially modify the accessibility of grain boundaries under repository conditions. The first one is linked to the helium accumulation in the ceramic and the second one to the water intrusion at the grain boundaries.

a) Concerning helium accumulation in the ceramic, a model recently developed under the European NF-PRO project (Ferry et al., 2007) is based on low helium mobility under alpha self-irradiation and a low helium solubility limit in the UO_2 grains. These hypotheses are supported by numerous experimental findings. This implies that the "only" process liable to modify the mechanical stability of the ceramic is the formation of helium bubbles a few nanometers in diameter inside the grains (or helium accumulation in preexisting fission gas bubbles) with increasing pressure in the bubbles leading to intragranular rupture. Rupture will occur above a critical pressure that depends on the tensile strength and porosity of the ceramic (Ferry et al., 2007) and will propagate to the grain boundaries, thereby increasing the surface area by several orders of magnitude and resulting in instant release. This model demonstrated that after 10 000 years the critical pressure will not be reached in the bubbles in the case of UOX spent fuel with a mean burnup of 47 GWd/t. This reassuring result can now be applied to the rim assuming a uniform distribution of pores with pore size ranging between 0.5 and 2.5 μm in accordance with literature data and a total porosity of 15% in the rim.

b) Concerning the second process, water will eventually penetrate the grain boundaries of multigrained specimens, thereby increasing the effective surface area. The amplitude of this phenomenon will depend on the nature of the spent-fuel, the local concentrations of oxidizing species, the duration of leaching...

Before discussing the operational aspects, it is important to reconsider and discuss experimental protocols and results.

A review of a large body of experimental data obtained for American ATM 104-105-106 fuel [2] showed that adding an uncertain and poorly controlled parameter—such as the surface area accessible to water (see discussion in chapter 2.2.1.2) —when calculating the leach rate or the normalized mass loss can lead to erroneous and meaningless differences in the release values. These differences can become imperceptible when the cumulative release fractions are compared (see figure 4).

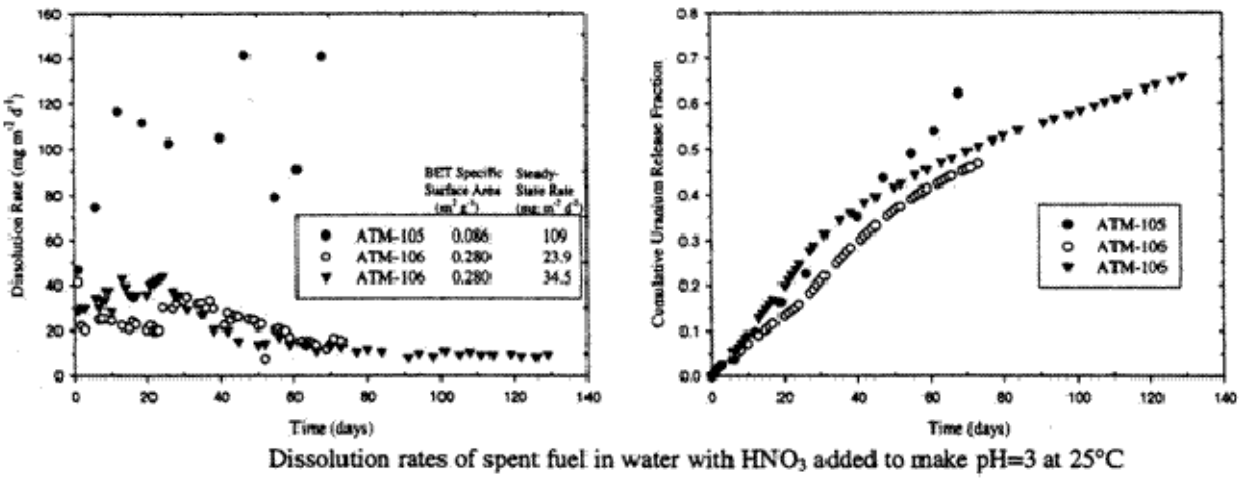


Figure 4: left: Disssolution rates of spent nuclear fuel samples of various specific surface areas, right: same data but expressed in terms of cumulative fraction of uranium release Hanson, and Stout [2]

Ideally, only samples with the same leaching history and origins should be compared to avoid any problem related to estimating the surface area accessible to water. It is therefore important to take care to the data representation modes and the nature (powder, fragments, etc.) and history (preleaching, washing, etc.) of the test samples before concluding and interpreting the results of experiments (Jégou et al., 2007). For example if all the fragments are sampled from the core of the same clad segment that had been leached for several months in an aerated water to eliminate the fission product inventories at the grain boundaries the specific surface area of all the fragments should be comparable. This remark suggests that the representation based on the release fractions should be used rather than the surface area normalized mass losses. In addition, calculating the normalized mass losses from the geometric surface area of the fragments does not make sense because it takes into account only the "external" surface area, which is not compatible with the sample leaching history. In other words, these fragments are more comparable to powder samples than to dense particles inaccessible to water. As the surface area is not accurately known, experimental data can thus be compared only in terms of release fractions and not of normalized mass losses. Except when "grain" specimens consisted of many thousands of separated grains from 7 to 20 μm in size are used, it is generally difficult to accurately determine the intrinsic dissolution rate of the fuel matrix, and any estimate based on the geometric surface area of the fragments would result in an unrealistic and probably overestimated bulk dissolution rate. Contrary BET method may overestimate the effective surface area by including some of the internal grain boundary surfaces that are not open to penetration by water (Gray and Thomas, 1994).

It is important to note that processes may also lead to a reduction in the **reactive** surface area (precipitation of secondary phases, diminishing reactive site density, etc.) as shown by several authors. Under strong oxidizing conditions even with an increasing surface area (opening of the grain boundaries…), the dissolution rates decrease when normalized to the fixed initial surface area. Various factors could be involved, including diffusive control of alteration, diminishing numbers of donor-acceptor sites for oxygen reduction, the presence of metal cations other than uranium on the fuel surface, and the semiconducting properties of UO_2. Under reducing conditions similar to those encountered in a repository site (European concepts) the accessibility of water at the grain boundaries is expected to be limited.

2.3.4 Uncertainties related to the radiolytical database (G-values etc.)

The yields of radiolytic species are given by so- called G-values. These values depend on the linear energy transfer (LET) values of the type of radiation, and are hence, quite different for low LET radiation such as gamma or beta radiation as opposed for high LET alpha radiation. The LET for alpha radiation increases with decreasing energy. We need to distinguish between the instantaneous LET valid for a given radiation energy value and the average LET, valid for an alpha particle of a given initial energy until its complete stop in the irradiated matter. The instantaneous LET for 5 MeV alpha particles is about 90 keV/µm but the average LET of a 5 MeV alpha particle until complete stop is 140 keV/µm. For spent nuclear fuel, alpha particles loose their energy to a large extend in the solid and only 10% of the alpha particles enter the solution with an initial energy > 4 MeV, more than 50% have energies lower than 2 MeV. This leads to average LET values for alpha radiation from spent nuclear fuel of about 170 keV/µm.

G-values in radiolytic models for spent nuclear fuel dissolution are in most cases used without uncertainties and without any reference to a choice of an average LET value. Literature values for the various radiolytic species were evaluated statistically in the project as a function of LET and a consistent set of G-values of 170 keV/µm alpha radiation has been derived together with associated uncertainties (see table.1)

Table.1 G values and uncertainties for alpha radiation with and average LET of 170 keV/µm

	H20	OH	H	H2	H2O2	H+	OH-	e-	HO2
Reference	-2.58	0.36	0.2	1.18	0.98	0.06	0	0.06	0.1
Uncertainty		0.1	0.2	0.1	0.1			0.06	0.03
Min	-2.4	0.26	0.13	1.08	0.88	0.12	0	0.12	0.13
max	-2.82	0.46	0.36	1.28	1.08	0	0	0	0.1

The propagation of these uncertainties to water radiolysis calculations has let up to 30% variation in calculated H_2O_2 concentrations.

.

2.3.5 Uncertainties in models describing the H_2 effect

2.3.5.1 Uncertainties in radiolytic models describing the H_2 effect

The study of the spent nuclear fuel behaviour under disposal conditions is usually based on the oxidative dissolution of the UO_2 matrix, in which oxidising conditions produced by water radiolysis are assumed. However, the presence of H_2 arising mainly from container and cladding corrosion, has been shown to inhibit the dissolution of the UO_2 matrix [59]. This phenomenon, which is expected to enhance the long-term stability of spent fuel, is referred to as "H_2 inhibition effect".

Some source term models do not take such inhibition effect into account, thus providing similar results for systems with high and low H_2 content. Such situation has been observed when the results of the modelling exercise in Work Package 3 have been analysed, e.g. identical results were obtained when the CEA model was applied to the Reference Case containing different initial H_2 concentrations [60]. However, the majority of radiolytic source term models intend to integrate the H_2 inhibition effect, all of them do it by considering that H_2 consumes the oxidant species in solution responsible for the oxidative dissolution of the matrix. According to this assumption, the higher the H_2 content, the lower the amount of oxidants in the system, and thus, the lower the oxidative dissolution of the matrix. Such assumption is intrinsic in the water radiolysis representation in three of the four source term models considered in Work Package 3, i.e. MAM, Maksima-trara and KTH models [**Error! Bookmark not defined.**]. However, even

though a H_2 inhebition effect is described in the models, additional information shows that it may nevertheless not always be described correctly:

- contrary to that predicted by the models, several radiolysis experiments of aqueous solutions have shown that under some conditions, e.g. alpha radiation field and absence of spent fuel, the presence of H2 does not considerably reduce the amount of oxidants, not even when H_2-saturated solutions are used [61]. This fact suggests that the radiolytic models do not properly describe the H2 inhibition effect, and thus, that the derived modelling results contain some inherent uncertainties. The project has shown that the main reason for the discrepancy between the modelling and the experimental results is that the radiolytic part of the H_2-inhibiting effect is strongly dose rate dependent [62]. In alpha radiolysis experiments only a very small fraction of the solution volume is exposed to the radiation energy, while in most modelling approaches, the same radiation energy is homogeneously distributed in the whole volume, resulting in dose rates several orders of magnitude lower than in the actual experiment. The impact of a given H_2-concentration increases with decreasing dose rate. At high alpha dose rates, the H_2 inhibition effect is insignificant. In order to better describe the purely radiolytic part of the H_2 effect, the actual dose rate profile must directly or indirectly be used in the source term models. This is done in the Maksima-trara model.
- several experimental studies have shown that ε-phase noble metal inclusions in spent nuclear fuel (or Pd particles in UO_2 pellets), efficiently catalyze the reduction of U(VI) by H_2 [63], which is a process not considered in most source term models. This process taken into account in the KTH model fully accounts for the H_2 effect observed for spent nuclear fuel The suggested impact of a UO_2 catalyzed reduction process is (if it exists) of insignificant importance for SNF dissolution.
- However an inhibition effect is also observed on alpha-doped UO_2. So the explanation of the catalytic effect of ε-phase noble metal inclusions does not describe sufficiently the inhibition effect.

2.3.5.2 *Uncertainties in electrochemical models describing the H2 effect*

As an alternative explanations of the inhibiting H_2 effect, the maksim-trara model uses an effect of H2 on reducing the corrosion potential. Experimental data show indeed that the corrosion potential decreases with H_2 and that this effect is more pronounced with an increased fraction of ε particles in the fuel. However, there are also large uncertainties in the electrochemical models as well as in the way of implementation in a code like maksima. Uncertainties occur also in electrochemical measurements.

Uncertainties in electrochemical measurements

Uncertainties in electrochemical measurements are strongly affected by the properties of the material and the system under investigation. When carrying out electrochemical experiments on UO_2 or spent fuel one has to consider first of all of course electrical and (electro)chemical properties of the material. A typical electrode made from a slice of UO_2 (spent fuel) can be seen as a metal electrode with an UO_2 spent fuel coating. Therefore an excellent sealing of the metal back-side is essential to avoid any contact with the test solution. Even a small pathway for the electrolyte is enough to falsify e.g. the measured open circuit potential by the corrosion potential of the metal in the electrolyte [64] .

Potential measurements can also be affected by the internal resistance of the measured object. UO_2 as semiconductor has a poor electrical conductivity and as a result a high ohmic resistance. Furthermore the electrochemical exchange current of UO_2 in aqueous media under anoxic or

reducing conditions is extremely small (nA and below). This requires for the potential measurement a voltmeter with a high input resistance (at least 10^{12} Ω) and the leakage current of the instrument should be negligible (pA-fA) compared to the exchange current. Also the input capacitance must be small (below 10^{-10} F) [65] [not to affect the potential. Under polarisation where the net current through the electrode is not zero an iR-drop of the potential occurs across the internal resistance of the electrode which has to be corrected.

Whereas the potential data provide mainly information on the thermodynamic driving forces of the reactions involved, kinetic information is retrieved from current measurements. Typical currents for the UO_2 system are below 10^{-8} A and therefore the ammeter must be sufficiently sensitive. But also the electrochemical system must be checked carefully especially at low concentrations (10^{-7}- 10^{-9} mol l^{-1}) of the potential-determining substances because the formation of the electric double layer can change the concentration in the solution. In case of low equilibrium concentration (e.g. formation of complexes or compounds of low solubility) of the potential-determining substances no deviation of the equilibrium potential is expected, because substance withdrawn from the solution will reform due to a shift in equilibrium. But in case of low absolute concentration the formation of the electric double layer will lower the concentration in solution and the potential will not be the equilibrium potential with respect to the original concentration [66].

Uncertainties related the question how microscopic behavior affects macroscopic observations

Additional uncertainties are caused by the heterogeneity of UO_2 and even much more of spent fuel. Sintered UO_2 is composed of grains, which have no preferred orientation, and grain boundaries in between. As a consequence electrical and chemical properties are not necessarily homogeneously distributed on the electrode surface. It was shown that in polarisation experiments on spent fuel, grain boundaries are preferably attacked [67]. Electrochemical atomic force microscopy has shown that local dissolution rates of UO_2 vary between different grain faces, grain boundaries and etch pits [68]. Quantum mechanical and empirical potential modelling of UO_2 surfaces have shown that the (111) surface has the lowest surface energy, followed by the (110) surface and the (100) surface [69]. These results show that the onset of corrosion in case of UO_2 and spent fuel is a local process which can occur at the various sites with different rates. Also the stoichiometry of UO_2 plays an important role. Under accelerated conditions, not relevant for disposal it was found that corrosion rate constants vary over a broad range determined by the degree of nonstoichiometry of UO_2 and the diversity of structures on the UO_{2+x} surface [70].

This leads to the question how these processes at the micro level are affecting the macroscopically measured properties. Also the surface area needs to be reconsidered (see also chapter 2.2.1.2). The electrochemically active surface area can be expected to be smaller than the wetted surface in contact with the solution. This may be one of the reasons why there is no direct proportionality between surface area and radionuclide release. In particular, the ratio of active surface area to total surface area may vary as a function of time. This could explain that even though surface area increases during leaching, corrosion rates decrease with time.

Uncertainties in electrochemical model implementation

In order to describe the oxidizing effect of radiolysis of water on the dissolution of UO_2 the maksima-trara model tries to couple the radiolytic model for water with a model for UO_2 dissolution based on an electrochemical approach.. This required formulating a number of additional reactions representing these electrochemical reactions, fictive species such as a concentration of electrons in UO_2 as well as dummy reactions to represent fractional reaction orders. These representations are calibrated with experimental data but application to experiments with H_2 implies extrapolation outside the calibrated range. Key result of model calculatins in the presence of H_2 is therefore not a prediction of a dissolution rate but the

demonstration that any oxidative dissolution rate would be so small that chemical dissolution of U(IV) under solubility controlled conditions would be the dominant dissolution mechanism.

2.3.6 Uncertainties on fuel dissolution due to the effects of near field materials

71

The near field materials that are considered most frequently in the disposal designs are metallic iron (inserts, container), cupper (container), and clayey backfill materials. The remaining free space in the waste canister can be filled with other materials (cast iron or steel, borosilicate glass, depleted uranium, dehydrated zeolites, hematite, spinel, olivine... [72], but the selection of these materials is still in progress. In the Belgian new reference design, the so-called 'Supercontainer Design', the near field will dominated by concrete, but this will still be separated from the fuel by a carbon steel overpack.

The effects of these materials have been treated only very partially in MICADO, via their effect on the solution composition and redox potential. The presence of steel has been included indirectly, because the steel produces Fe(II) and H_2 gas, which play a role in the radiolytical schemes used to calculate the oxidative fuel dissolution. Clayey materials are also expected to have an effect on the redox conditions, because they often contain traces of pyrite. Clays and metallic corrosion products are, however, expected to have an influence on the fuel dissolution also by sorption of U species. The sorption of U(VI) can probably be considered as a secondary effect without much impact on the fuel dissolution rate. The sorption of U(IV) could, however, trigger the non-oxidative fuel dissolution until the sorption sites are saturated [73]. The non-oxidative dissolution has hardly been treated in WP1, 2 and 3 of MICADO, because the modeling was focussed on test conditions in absence of materials with a uranium sorption capacity. In such conditions, equilibrium of U(IV) (in reducing conditions) with the fuel surface is reached very soon, after which the system can be described by solubility, rather than by dissolution kinetics. Solubility constraints for U(IV) were not studied in MICADO since detailed studies are available.

So, although the total fuel dissolution can be described as the sum of oxidative U(VI) dissolution and non-oxidative U(IV) dissolution, MICADO has focussed only on the kinetics of the oxidative term. A non-oxidative kinetic term may additionally become relevant only in the presence of near field materials with a strong sorption capacity in very close vicinity to the fuel , or when saturation is prevented by very fast water flow with a low natural U(IV) background concentrations. Natural background concentrations of Uranium in granitic or clay waters are between 10^{-8} and 10^{-10} M. Few tests have been done to study the sorption effects of clayey materials or other potential near field materials on the UO_2 dissolution. Hence, the database is relatively small. There is, however, enough evidence from tests with Boom Clay that UO_2 dissolution can indeed be triggered by U(IV) sorption on the clay [71] , although there are still some uncertainties about the precise mechanisms (the conceptual model). The uncertainty about the model parameters is still considerable.

The most important arguments that support the hypothesis of accelerated U(IV) dissolution in the presence of Boom Clay are the following:

- In tests with Boom Clay, the total amount of U released from the UO_2 in the first leaching period is much larger than in tests without Boom Clay. Because Boom Clay is a reducing medium, there is no reason why it should accelerate the oxidative dissolution. It is more plausible to suppose that it accelerates the non-oxidative dissolution.

- In tests with Boom Clay, the dissolution rate of alpha doped UO_2 did not increase with alpha activity. If radiolytical oxidation would be the dominant dissolution mechanism, one would expect to see a higher dissolution rate (and more uranium sorption) for the more active UO_2.
- Sequential extractions of Boom Clay that had been exposed to UO_2 for a long time have revealed that the vast majority of the released uranium is associated to the organic fraction of the clay. Literature provides much more evidence for sorption of U(IV) on organic matter, than for sorption of U(VI).

The conceptual model for fuel dissolution in contact with reducing clayey materials (such as Boom Clay) , would describe the fuel dissolution in four stages:

- A first short period with a strong rate increasing effect of the clay, is a combination of simultaneous non-oxidative and oxidative dissolution. The non-oxidative term (U(IV) release) is driven by sorption on the clay (possibly the immobile organic matter is a sink), whereas the oxidative term (U(VI) release) is due mostly to dissolution of a possible preoxidised layer.
- The second period is marked by a strong decrease of the dissolution rate. The decrease of U(VI) release would be attributed to exhaustion of the preoxidised layer. The decrease of U(IV) release would be due to the saturation of nearby U(IV) sorption sites of the clay.
- The third period is characterized by a constant oxidative dissolution, resulting from the alpha-radiolysis, with possibly a small non-oxidative term due to continued, slow U sorption on the clay.
- When the alpha-activity becomes lower than the threshold for oxidative dissolution, the oxidative dissolution would stop, and only non-oxidative fuel dissolution continues. We would have a solubility and diffusion driven non-oxidative dissolution rate. This would be the fourth stage, but the experiments in the presence of clay did not clearly demonstrate the existence of this stage.

In this scheme, release of U(IV) driven by sorption on near field materials will be potentially important in the first stage, but its long term importance is in the fourth stage, when non-oxidative fuel dissolution is the only dissolution mode. The dissolution of U(IV) is expected to slow down quickly (second stage), after saturation of the nearby sorption sites. Because of the low solubility of the U(IV) controlling phase and the diffusion controlled transport in the near field, a solubility-sorption-diffusion model seems appropriate to describe the evolution of the non-oxidative dissolution rate. This non-oxidative term should be added to the oxidative fuel dissolution term, which has been studied extensively in MICADO. The parallel oxidative dissolution rate would not be influenced by the presence of clay, or in a favourable way, because the clay provides reducing conditions, which can increase the threshold for oxidative dissolution. Oxidatively dissolved U(VI) is expected to become reduced also on the pyrite of the clay, but this should not have an impact on the oxidative dissolution rate.

Unfortunately, the reproducibility of tests with UO_2 in clay media is poor. For this reason, it is difficult to prove that the UO_2 dissolution is indeed solubility controlled after saturation of the clay. For this reason, the fourth stage needs further confirmation.

The parameter values necessary to describe the transport (sorption and diffusion) of U(IV) in compact clay are not well known.

- The retention of U(IV) in Boom Clay as observed in column migration experiments is relatively small (retardation factor R of 95 [74]), while batch sorption tests with U(IV) and tests with the analogue Th(IV) indicate a high sorption. The relatively low retardation in the column experiments was attributed to colloid formation and

subsequent migration while the batch experiments reflect more the sorption of non-colloidal U(IV) species. The low retardation can be used in performance assessment because it is conservative with regards to the migration rate. If, however, sorption of U(IV) accelerates the fuel dissolution, than one should use the more realistic higher retardation factors to model the source term, and these are not well known.

- The diffusion coefficient of U(IV) is difficult to measure directly with U(IV). Pessimistic estimations are made, using the diffusion coefficients of unretarded species (tritium, iodide). For the coupling with fuel dissolution, this assumption is equally pessimistic.
- The maximum sorption capacity of Boom Clay for U(IV) is important, because the non-oxidative fuel dissolution would stop when this capacity is reached. Its value is, however, not well known. Depending on the test conditions, average values up to 15 µg U per g of clay were reached in tests with clay and UO_2 (with peaks up to 70 µg/g), after which there is no further increase [71]. The sorption capacity depends on the clay characteristics, and may depend for instance on its organic matter content. Tests with the analogue thorium (Th(IV)) have been performed as well. In these tests, the amount of thorium found per gram of Boom Clay was up to two orders of magnitude higher than in tests with UO_2, but the test conditions were different (much lower solid/liquid ratio for the thorium tests).
- The uranium solubility in clay conditions is known within certain ranges. The uranium solubility for doped UO_2 in Boom Clay conditions was in the range 10^{-9} to $4.7x10^{-8}$ Mol/L. This can correspond to equilibrium with a U(IV) phase such as UO_2(am) or $UO_{2.333}$. The presence of the clay does not seem to have much impact on the dissolved (ultrafiltered) concentrations, so the solubility controlling uranium phase may be the same as in absence of clay. The organic matter can however increase the mobility of U(IV) by colloidal interaction.
- Because the dissolution is solubility controlled, the exposed surface area of the fuel is no relevant parameter for the U(IV) release.
- The parameter values can be different for host rock clay, like Boom Clay, and backfill bentonites. The available data should be evaluated individually.

Little is known about the influence of the other potential near field components, but it is likely that they will have an effect on the fuel dissolution rate mostly also by sorption or immobilization of U(IV). The net effect and mechanisms may, however, be different.

The near field materials will have still other effects:

- Their reducing properties may help to limit the radiolytical oxidation, even in absence of H_2 gas.
- The near field materials might have a negative impact if the sorption of dissolved uranium on their surface prevents the formation of secondary uranium phases on the fuel surface. The formation of such phases on the fuel surface could have a protective effect. On the longer term, when the first layer of the near field is saturated with released uranium, we can however still expect secondary phase formation at the interface fuel/near field. So, this effect is probably not important on the longer term.

Conclusions and relevance for PA:

There is evidence that sorption of U(IV) on near field materials can cause an acceleration of the fuel dissolution. The short term effect will be difficult to quantify, because the characteristics and evolution of the metallic layers and the filling materials, which will be the first layer in contact with the fuel, cannot be predicted well enough. The long term effect, with UO_2 dissolution controlled by U(IV) diffusion into the bentonite or host rock, can be modeled in a

more robust way. It will, however, be necessary to carefully select the transport related parameters for U(IV), because the uncertainty about their values is still large. Conservative assumptions have to be made to compensate for the model uncertainties.

2.3.7 Uncertainties relative to users of models

The uncertainties pointed out can be summarised as follow:

- There are no published manuals for the codes, with clear user instructions. The users could find only manuals,describing the procedure for data input, explaining the mathematical approach for resolving the differential equations and the explaining the meaning of the output file.

- None of the models has an easy and/or user-friendly interface. Often, it is necessary to perform mathematical operations to obtain the necessary parameters for the input files (normally, ASCII format). These mathematical operations are often the only way to provide key input parameters such as specific surface area, site density, S/V ratio and other geometric parameters. Such procedures are a source of error.

- Mathematical treatment is also needed on output files (usually as concentration) in order to obtain the matrix alteration rate and or % of altered mass.

It would be useful to develop a tutorial to work with the codes relevant for the scientific community. This fact could increase the understanding of each model by other users and help to implement and promote the collaboration between different research groups.

2.3.8 Proposition of a bounding case matrix dissolution rate in presence of hydrogen

FZK [29,34] has measured with high burnup fuel (50 GWD/tU) in presence of corroding Fe a dissolution rate of 1E-9/day after 4.5 years. The iron corrosion has led to the buildup of hydrogen pressures in the autoclave. The rate value can be translated to a surface area nomalised value using an appropriate choice of a specific surface area value and resulting rate values are directly correlated. The experimental value is only $1.0 \cdot 10^{-9}$/day (based on Sr release). With minimum accessible surface area (SA_{min}) of 0.001 $m^2 \cdot g^{-1}$ (chapter 2.1.2) this corresponds to a surface area normalized reaction rate of 1 $\mu g \cdot m^{-2} \cdot d^{-1}$ and with the maximum accessible specific surface area (SA_{max}) of 0.0071 $m^2 \cdot g^{-1}$ this corresponds to 0.1 $\mu g \cdot m^{-2} \cdot d^{-1}$.

Rölin et al. [5] performed flow through experiments with fuel of an average burnup of 43 GWd/tU in H_2 atmosphere and measured a dissolution rate of about (3±2) $\mu g/m^2 d$. Werme et al. [75] interprets this value as too high since the H_2 flow rate might have been too slow to block all radiolysis effects. Nevertheless, for the present evaluation this value is kept in the assessment of uncertainties.

In conclusions one could say that the choices for rate values in presence of hydrogen for SA_{min} are between 0.2 and 5 $\mu g \cdot m^{-2} \cdot d^{-1}$ and for SA_{max} between 0.02 and 5 $\mu g \cdot m^{-2} d^{-1}$.

2.4 PERIOD BEYOND HUNDREDS OF THOUSANDS OF YEARS : FUEL MATRIX DISSOLUTION UNDER REDUCING CONDITIONS WITHOUT HYDROGEN GAS

2.4.1 Evidence of UO_2 stability under reducing conditions from natural analogues

The observations of long-term stability of natural uraninites provide some insights regarding how spent fuel may behave in a repository in the period beyond several hundred thousand years after disposal, a time beyond which the activity of the fuel is approaching that of a rich uraninite ore. As such, it can be argued that the insights from these studies complement the information from radiolytic and electrochemical models related to spent fuel examined in the MICADO Project and provide confirmation of some of the basic elements of these models. In particular, the studies provide a basis for the argument that there is a threshold of specific activity below which uraninites are thermodynamically stable in a reducing environment and thus may be experiencing dissolution principally as U(IV). Some aspects related to the long-term stability of uraninites are discussed below.

Characterization of uranium minerals indicates that uraninite is the most common uranium phase in nature under reducing or anoxic conditions. Uraninite has a defective fluorite structure with a nominal composition of UO_{2+x}, $0.01<x<0.25$, in which excess oxygen is balanced by oxidation of some of the U(IV) to U(VI). Evidence indicates that this mixed U(IV)/U(VI) composition arises during ore formation and is not the result of subsequent oxidation. However, it has been shown that natural uraninites may contain significantly more U(VI) in the lattice than the composition above suggests, which may be explained by substitution of other cations in the lattice [79]. This leads to some difficulty in applying thermodynamic data for UO_2 to natural uraninites and strict comparisons between uraninite, spent UO_2 fuel and unirradiated UO_2 are difficult [76]. Good arguments have been made that uraninites and spent UO_2 fuel are more similar to each other than are spent UO_2 fuel and unirradiated UO_2 [77], including similarities in structure, resistance to radiation damage, oxidation behaviour, solid solution behaviour (e.g. with Th and lanthanides) and fission product behaviour (in the case of the natural fission reactors at Oklo). .

Despite the observations of uraninite stability, it may be partially converted into other uranous minerals while reducing conditions are maintained [78]. Coffinite, i.e. $U(SiO_4)_{1-x}(OH)_x$, is the most reported U(IV)-altered mineral in natural uraninite samples. For instance, characterization work carried out on Cigar Lake samples indicates the coexistence of fine grained coffinite, uraninite and quartz [79]. Although thermodynamic data indicate that coffinite is formed at [Si] $> 10^{-3}$ M and reducing conditions [80], which is compatible with the Si concentrations determined in the coffinite environments of Oklo and Palmottu ($5\cdot10^{-3}$ to 10^{-2} mole·dm^{-3}), it has not been possible to experimentally reproduce coffinitization of uraninite under such conditions. This fact indicates either that unknown factors must be fundamental for the transformation of uraninite into coffinite, or that there is a lack in the coffinite thermodynamic database or that the process occurs extremely slowly and is difficult to reproduce in the laboratory. It is difficult to assess the significance of coffinitisation in relation to the disposal of spent fuel. It should nonetheless be noted that even if it is an ongoing process in uraninite deposits such as Cigar Lake, and it is likely that alteration occurred principally at temperatures above 100°C [81], rather than the ~20-50°C range expected for repositories in the post-canister failure stage, the rate of alteration must be every low as the deposit is primarily uraninite and has an age of ~1.3Ga.

Although U-mobility from U(IV)-solid phases can be increased under some naturally occurring conditions (e.g. CO_2-rich fluids has shown to mobilise uranium from the sediments of the Liueryiqi granite-hosted uranium deposit [82]), reducing conditions are able to keep U-mobility at minimum, as it is shown by the persistence over very large periods of time of uraninite ores, even in cases where contact with significant water flow has taken place (Cigar Lake, Oklo, etc).

The extent to which radiolysis may have influenced uraninite stability was considered in some detail in the Cigar Lake Project [83,84]. The conclusion was that oxidant production from radiolysis may have been largely neutralized by oxidation of sulphides and possibly reactions with the uraninite, but that oxidative dissolution has not occurred. The radiolytic models used in reaching these conclusions were considered to be realistic to conservative in their predictions of the amounts of oxidants produced [84].

The observations of the stability of uraninite over geological time provide only qualitative and semi-quantitative indications of the long-term stability of spent fuel in a geological repository. The direct application of such observations to performance assessment models in any quantitative sense is difficult and has not been achieved despite extensive efforts. However, these observations are useful in building confidence for performance assessment for disposal of spent fuel, in particular for the period beyond several hundred thousand years after disposal of spent fuel. In this time period, the alpha-emitter content of spent fuel has decayed to a level approaching that of rich natural uraninite ores. As the dissolution rate of natural uraninites must be extremely low under reducing conditions or they would not be preserved over geological time, the dissolution rate of spent fuel after several hundred thousand years would likewise be expected to be similarly low in a reducing geological environment.

2.4.2 Uncertainties in radiolytic models close to or beyond dose threshold, including the effect of Fe^{2+}.

Most source term models are based on the radiolytically-mediated oxidative dissolution of the spent fuel matrix [85]. These models consider that the residual activity of the spent fuel will produce oxidants through water radiolysis, which will be responsible for the oxidative dissolution of the matrix. According to these models, the lower the dose, the lower the concentration of oxidants and, as a consequence, the slower the spent fuel dissolution rate. In the limit, when the dose is insignificant, the dissolution rate predicted by the models approaches zero. Such relation between dose and dissolution rate has been observed when different source term models were applied to different systems in the framework of Work Package 3 [86]. In this modelling exercise, uranium concentrations as low as $3 \cdot 10^{-13}$ M were predicted, *e.g.* when modelling the MDR_02_ITU_S with Maksima-trara model, which is even lower than the solubility of the UO_2 matrix.

In fact, experimental results have shown that radiolytic dissolution is the controlling mechanism down to a dose threshold, below which solubility-controlled processes become predominant. Such processes make reference to the intrinsic solubility of the non-oxidised matrix, *i.e.* solubility of U(IV), which at specific activities lower than the dose threshold, produce residual dissolution rates larger than those due to radiolytic processes. The dose threshold itself depends on environmental parameters such as the redox conditions of the media [87]. Under the expected reducing conditions induced by accumulation of H_2 and Fe^{2+} (derived from corrosion of the iron of the canister), the specific activity threshold will be in a range of some hundreds of megabecquerels per gram of UO_2 [**Error! Bookmark not defined.**]. Since such dose is lower than the fuel activity after canister failure (around $2 \cdot 10^4$ years), the matrix alteration rate

is likely to be controlled by the solubility of the non-oxidated matrix from the very beginning of the water intrusion process.

Most radiolytic models do not consider the solubility of the non-oxidized matrix, and thus, they probably underestimate the matrix dissolution rate in the long term, in which low specific activity and reducing conditions are expected. In order to improve these models, a threshold matrix dissolution rate should be considered in all cases, which in addition, should depend on the solubility of $UO_2(s)$ under the chemical conditions of the media, *e.g.* Eh, $[Fe^{2+}]$, $[H_2]$, $[CO_3^{2-}]$, *etc*.

2.4.3 Uncertainties in electrochemical models

Uncertainties are similar to those described in section 2.3

2.4.4 Uncertainties on fuel dissolution due to the effects of near field materials

Uncertainties are similar to those described in section 2.3

2.4.5 Proposition of a bounding case matrix dissolution rate under reducing conditions (or range) in the absence of hydrogen gas

Although a number of works have studied the $UO_2(s)$ dissolution under oxidising conditions [88], less attention has been paid to the study of the $UO_2(s)$ dissolution in reducing media [89]. However, the latter conditions are of utmost importance in the long term after about 10^5 yr, where reducing conditions prevail, even when corrosion of the iron-based canister is terminated (via natural geochemical reduction capacity, presence of accumulated of Fe^{2+}). The remaining radioactivity of the fuel is expected to induce only a very mild oxidizing effect so that oxidizing dissolution rates become lower than those associated to the chemical, non-oxidizing dissolution of the $UO_2(s)$ matrix itself, the latter becoming the main dissolution path. Hence, having reliable data on matrix dissolution rates under reducing conditions seems to be vital in all performance assessment exercises.

We can expect that the spent fuel matrix will be close to thermodynamic equilibrium in reducing conditions, when self-oxidation becomes negligible. If the matrix is in equilibrium with the solution, there should be no net remaining matrix dissolution. Nevertheless, the non-oxidative matrix dissolution might continue because of conversion to other, more stable U(IV) minerals, like observed for natural analogues (section 2.4.1), or because of sorption of dissolved U(IV) on near- (and far-) field materials (section 2.3.6). Hence, a residual non-oxidative dissolution cannot be excluded, but the dissolution rate should be very small. In principle, one expects a coupling between the U(IV) dissolution and its removal via secondary phases or sorption. These processes are, however, very difficult to quantify.

Few studies deal with the kinetics of dissolution of $UO_2(s)$ under reducing conditions, which is due to the difficulty of maintaining reduced the whole $UO_2(s)$ surface, thus avoiding that other than the non-oxidative dissolution of $UO_2(s)$ are the main mechanisms responsible for the matrix alteration and uranium mobilisation [90]. One of the first studies of the kinetics of dissolution of $UO_2(s)$ as a function of pH under reducing conditions ($H_2(g)$/Pd) was performed by Bruno et al. [**Error! Bookmark not defined.**a, 5b]. The authors found dissolution rates up to $36\pm16\ \mu g\cdot m^{-2}\cdot d^{-1}$, which is much higher than the rates reported afterwards by other authors for reducing conditions, even in absence of hydrogen gas. It is possible that the dissolution rate was increased by the continuous solution renewal applied to remove the oxidized surface layer (dynamic tests).

Other dynamic tests in reducing conditions were performed by SCK•CEN in the SFS project. The dissolution rates for alpha doped UO_2 were between 1 and 245 $MBq\cdot g^{-1}$ where in the range

between 0.7 and 2 $\mu g \cdot m^{-2} \cdot d^{-1}$ (see SFS deliverable D9). Although these tests were performed with a naturally reducing ground water (Boom Clay water, with high concentration of HCO_3^- and organic matter), the uranium in solution was probably still predominantly U(VI), and hence the result of a residual oxidative dissolution. Non-oxidative dissolution was likely to take place also, but the U(IV) dissolved from the UO_2 surface probably reprecipitated on the cell wall before it reached the outlet. The amount of uranium on the cell walls, measured after the tests were stopped, was relatively large, and is probably a better indication for the non-oxidative dissolution rate than the uranium that remained in solution. The average dissolution rate of U(IV) dissolution corresponding to the mass of uranium found on the cell wall was between 1 and >30 $\mu g \cdot m^{-2} \cdot d^{-1}$. So, relatively high non-oxidative dissolution rates occurred, but these cannot be considered as an intrinsic material constant. They are rather maxima, influenced by the dynamic experimental conditions. Extrapolation to the static *in situ* conditions would be overconservative.

Static dissolution tests with alpha-doped UO_2 in reducing Boom Clay suspensions suggest a dissolution rate of 7.2 ± 7.8 $\mu g\ m^{-2} d^{-1}$, independent of the alpha activity, and hence probably at least partly caused by non-oxidative dissolution [71]. In these tests, the non-oxidative dissolution rate may have been increased by the availability of sorption sites for U(IV) on the suspended clay particles.

From static dissolution tests in reducing conditions, using ^{233}U doped UO_2 [91] one deduces after 52 days of leaching a dissolution rate of $(8.5 \pm 4) \cdot 10^{-8}$/yr corresponding with SA_{min} to $(0.24 \pm 0.12) \mu g \cdot m^{-2} \cdot d^{-1}$ and with SA_{max} to $(0.03 \pm 0.015) \mu g \cdot m^{-2} \cdot d^{-1}$.

In other static dissolution tests dissolution experiments with alpha doped UO_2 using the isotopic dilution method, (NF-PRO, final synthesis report, p. 67 (2008)) Ollila found under reducing conditions a dissolution rate between 0.5 and 2.6 $\mu g \cdot m^{-2} \cdot d^{-1}$, even though total U concentrations remained constant. However, these values must be considered as maximum values, considering that ongoing isotopic exchange considers only the outermost surface of the UO_2 and it is doubtfull that isotopic exchange will continue for all atomic layers beneath the surface.

Because the long-term non-oxidative dissolution rate expected *in situ* is best approached by static conditions in absence of surfaces for sorption, residual rates between 0.03 and 2.6 $\mu g \cdot m^{-2} \cdot d^{-1}$ can be proposed for reducing conditions at near-neutral pH. In an alternative approach, a solubility/diffusion/sorption driven model can be used to describe the non-oxidative dissolution rate. The corresponding long term rate (after saturation of the near-field) will be lower than the constant residual rates proposed higher.

Integrating the proposed matrix dissolution rate in some modelling exercises performed in the framework of WP3, could be used to overcome some limitations inherent in the source term models used [92]. For instance, when MAM and Maksima-trara models were applied to some UO_2(s) dissolution experiments under H_2 media and low dose rates, e.g. MDR_02_ITU_S dataset, the estimated uranium concentrations are much lower than the experimental ones, as none of these models takes into account the direct dissolution of the reduced matrix [93]. If the above-mentioned dissolution rate had been considered in the calculations, the estimated uranium concentration would have been of the order of 10^{-9} M, which are actually the ones experimentally determined.

3 Consequences of uncertainties in fuel dissolution modeling on confidence in assessment of overall repository performance

3.1 SP1

In the framework of WP4, Andra has performed modeling calculations in order to review and evaluate in a performance assessment context the influence of uncertainties associated to about 20 parameters: ~5 input data of source term models (IRF, UO_2 dissolution rate, U solubility, specific surface area, corrosion rate of zircaloy) and ~15 parameters associated to the materials present in the repository environment (hydraulic parameters, transfer parameters of EBS, backfill in gallery, COX).

Two highly mobile long-lived radionuclides of interest for PA have been considered for these calculations: one fission product I-129 and one activation product Cl-36. Their release was described by the instant release fraction (IRF), a slow long-term release due to the dissolution of the pellet matrix and, for chlorine, by the corrosion of metallic structural elements such as zircaloy cladding.

Regarding the spent fuel source term, radiolytic dissolution is expected not to be the dominant process in the long term, considering in particular the canister lifetime (10 000 years at least, guaranteed per design), and the current state of knowledge on the production of H_2 and its effect on radiolytic dissolution (H_2 inhibition effect). That's why the partners involved in the WP4 have decided to focus on two source term models : a model based on the matrix dissolution under reducing conditions with very low dissolution rates (ranging from 0.2 to 5 $\mu g.m^{-2}.d^{-1}$)and a model based on the U solubility (ranging from 10^{-10} to 10^{-7} M).

A physical/statistical analysis in time and space based on PA indicators (molar rates through 8 surfaces from the wastes packages to the top and bottom of clay layer) both in near and far field have allowed us :

- to better understand this multiparametric system (source term and porous media) in a PA approach.
- to identify the relevant input data whose uncertainty control the uncertainty of the results.

The obtained results are valid both for I-129 and Cl-36. The single particularity of chlorine is the fraction released by corrosion of zircaloy. It appears that the release rate is much smaller than the inverse of travel time from waste packages to gallery. Consequently, the fraction of chlorine released by corrosion is viewed as labile and associated to the IRF by the different PA indicators.

As regards the rate control model, the results show the influence of the IRF on PA indicators in the near field (up to 3 meters around waste packages), as well as the distribution coefficient (Kd) and the effective diffusion coefficient (De) of bentonite. But above all they point out the influence of the dissolution rate and the specific surface area of the matrix for all PA indicators. For PA indicators in the far field, the Kd of COX and hydraulic parameters of COX have also an influence.

As regards the U solubility control model, the relevant parameter is is IRF which controls all PA indicators due to the very low matrix dissolution rate (< 1.2 10^{-9} $year^{-1}$) whatever the value of the U solubility in the variation range studied. In 1 million years (duration of calculations), less than 0.1 % of the nuclide initial inventory has been released out of waste package by matrix dissolution.

For the two models, the analysis of PA indicators show a large dispersion of results, which is due to both the dispersion of diffusive travel times ranging from 10^6 to 10^9 years and of matrix release rate ranging from 10^{-7} to 8 10^{-6} $year^{-1}$ (only for the rate-control model).

3.2 SP2

Within the MICADO project, SP2 has assessed the influence of spent fuel degradation models on radionuclide migration in the near and far fields of a deep underground repository for nuclear waste, based on the regulatory viewpoint. An important part of this work was i) to identify the uncertainties and assumptions made in simulating the spent fuel degradation and ii) to assess the consequences of these on the release of radionuclides from such disposal facilities.

For this purpose, radionuclide transport modelling and calculations of the activity fluxes from waste canisters to the near field (around the disposal tunnel or hole) and far field (host rock boundaries) were carried out. The computational models were based on repository concepts for both clay and granite host rocks. Characteristics of the models and near field environmental conditions were derived from the repository design developed by national operators; from France for the clay host rock (horizontal disposal tunnel connected by drifts), and from Sweden for the granite concept (vertical deposition holes connected by a horizontal access tunnel). A different conceptual model was developed for each of the two concepts and each was implemented in a separate computer code, Melodie and AMBER for the clay and granite host rocks respectively. Deterministic and probabilistic approaches comprise a simplified radionuclide source term composed of three parameters to represent activity release from the spent fuel: the instant release fraction (up to 10% of the initial inventory in the clay case), the dissolution rate (ranging from 10^{-8} to 2.5 10^{-5} y^{-1} depending on rock type and dissolution processes, i.e. radiolysis or uranium solubility control) and the inventory. A broad list of radionuclides has been taken into account in the calculations from soluble and non-sorbed anions (I-129, Cl-36, C-14) to decay chains (e.g. U-238 chains).

The conclusions from the results of the calculations carried out under the MICADO project differ depending on whether the repository is placed in a clay or a granite formation.

Simulations of the clay formation suggest that the matrix dissolution rate and the instant release fraction (IRF) are the main parameters determining the flux of radionuclides on the scale of the near and far fields. The scenario studied shows that the IRF determines the initial level of the activity flux in the near field if the radionuclide (e.g. I-129, Cl-36, C-14) is not immediately precipitated or sorbed in the vicinity of the canisters. The dissolution rate determines the level of activity flux out of the disposal tunnel or hole in the long-term (e.g. I-129 for clay, Ra-226 for granite). The transfer time throughout the host rock smoothes the activity fluxes by broadening the radionuclide plume. Because of the larger amount of total activity in the fuel matrix compared to the IRF, the dissolution rate clearly determines both the time of the peak and its magnitude at the host rock outlets in the long term.

These conclusions on the importance of the radionuclide source term in the clay formation agree with other international projects or performance assessment studies. For example, under the NF-PRO project, it was stressed that the impact of a repository closely depends on the mechanism controlling the matrix dissolution and to a lesser extent on the IRF by only testing different rates of release (all other parameters being identical). In addition, the present results for the clay formation refine those conclusions by sampling wide ranges of values for the three parameters characterising the source term (as illustrated in Figure 6). The uncertainty in the activity flux (which is within a range of one order of magnitude) is strongly correlated with the uncertainty associated with the values of those three parameters (e.g. correlation coefficient greater than 0.8 in Figure 5 and 6).

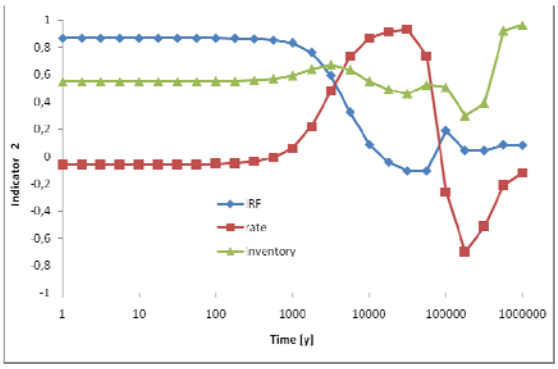


Figure 5. Correlation coefficients as a function of time for activity flux leaving the tunnel by the plug (clay-rock model)

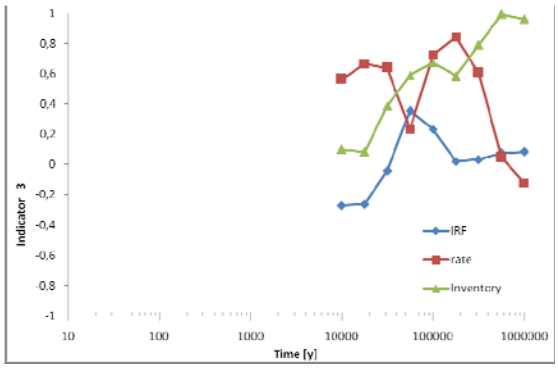


Figure 6. Correlation coefficients for activity flux at the top of the host rock (clay-rock model)

However, it remains difficult to draw strong conclusions on the real impact of the individual parameters. It would be useful as a first step to determine a better probabilistic density function for each parameter. A further refinement of the model for the source term and its parameters would improve the understanding of the repository behaviour.

For the granite concept, the source term parameters are found to be not as important as the flow in fractures intersecting the deposition hole. Whilst, as in the clay concept, the IRF determines the initial level of activity and the matrix dissolution rate the long-term levels, the peak flux contributed by the IRF is generally larger than that produced by dissolution of the fuel matrix (except in a few cases in the sensitivity study with very high dissolution rates and very low IRFs). Within the regulatory timescales therefore, the IRF is the most important parameter of the two for the granite concept. However the uncertainties in these parameters have rather less bearing on the range of peak fluxes calculated in sensitivity studies than in the clay concept. This can be seen from the scatter plots presented in**Error! Reference source not found.** in Fig. 7 and in Fig. 8, showing the fuel dissolution rate and the equivalent flow rate in a fracture intersecting the deposition hole plotted against the peak total flux (the main pathway for radionuclides leaving the repository). However, it is only true that the fuel dissolution rate is unimportant in the case where the bentonite buffer surrounding the canisters remains intact and the transport of radionuclides through the near field is diffusion limited. In this respect, it would appear to be of more importance to reduce the uncertainty in the understanding of the groundwater flow near deposition holes (including the effectiveness of the buffer as a flow barrier) rather than the source term for the granite concept. For the clay concept, uncertainty associated with sorption and precipitation in the host rock and uncertainty in the sealing performance also put into perspective the importance of source term parameters.

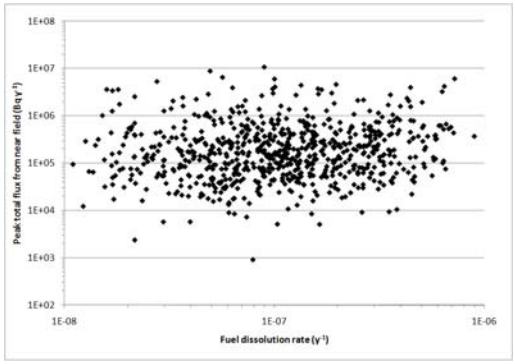


Figure 7: Scatter plot of the fuel dissolution rate vs. the peak total flux from the near-field (granite-rock model).

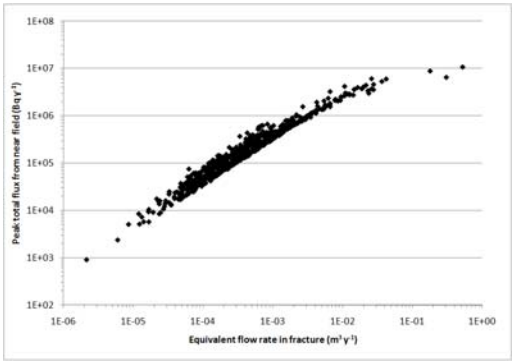


Figure 8: Scatter plot of the equivalent flow rate in a fracture intersecting the deposition hole vs. the peak total flux from the near-field (granite-rock model).

Effect of environmental conditions

Further calculations carried out by SP2 studied the impacts of environmental conditions corresponding to expected or postulated evolution scenarios influencing the release of radionuclides.

In this respect, calculations addressing different environmental conditions in the near field of the canisters have been carried out to determine the possible influence of those conditions on the release and transfer of activity. The composition of pore water leaching the UO_2 matrix is assumed to influence the release of radionuclides from the pellets. Therefore, several pore water compositions were proposed for environmental conditions which might be encountered in a geological disposal, i.e. a base case with water in equilibrium with host rock and so-called hereafter "alternative" cases (alkaline water, glacial melt water, and water encountering oxidative or thermal perturbations). Such environmental conditions were assessed as "what if" scenarios, the results would thus need to be taken cautiously.

In the clay concept (Figures 9 and 10), for all the alternative cases the fuel dissolution and activity flux results are strongly increased compared to the base case (red curve), even when the perturbation duration is negligible compared to the evaluation duration (100-year duration for oxidative perturbation). The conditions associated with those cases lead to a range of up to 9 orders of magnitude. However, in spite of the high gaps between the cases, the results remain lower than those obtained when using a simplified radionuclide source term from the first set of calculations (called conservative case in Figures 9 and 10). The fluxes obtained with a source term only composed of the IRF are higher than those of the base and alternative cases, which show the importance of determining that parameter precisely. The IRF value may allow the quantification of the minimum flux contributing to the impact of a repository, when fuel dissolution processes lead to a very low release rate.

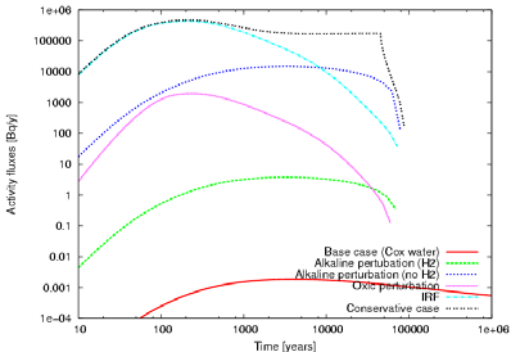


Figure 9. Evolution with time for activity flux leaving the tunnel by the plug (clay-rock model)

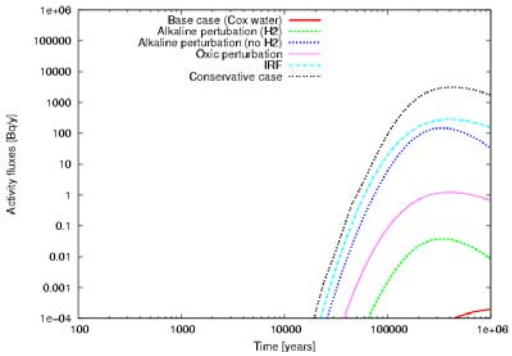


Figure 10. Evolution with time for activity flux at the top of the host rock (clay-rock model)

For the granite concept the alternative scenario considered was a case where glacial meltwater erodes the bentonite buffer, exposing the canister to advective flow. As with the clay concept, this led to elevated fuel dissolution rates and subsequently to elevated activity fluxes leaving the near field. Unlike the base case scenario where the bentonite buffer remains intact and limits the transport of radionuclides away from the deposition hole, here there are no such restrictions. Consequently the peak flux is linked intimately to the fuel dissolution rate, and it is this parameter that has the greatest influence on activities in the near field rather than the IRFs.

The present sensitivity analysis has been performed using outputs from a single detailed dissolution model provided by SP1. Other dissolution models have also been presented within MICADO which could offer different views on dissolution rates. The benchmarking undertaken for this project by SP1 partners shows that, for the same set of data, results differ from one model to another. The use of the complete set of dissolution models would therefore allow refinement of the range of possible impacts for each of the expected or postulated environmental conditions.

3.3 CONCLUSIONS

Different transport models (2D, 3D, PA-style) have been used by SP1 and SP2 to determine the effects of the fuel dissolution rate on the activity fluxes released by a nuclear waste repository. A broad list of situations has been simulated in order to highlight the importance of this parameter on the release and the migration of radionuclides through the repository components. For instance, fuel dissolution models based on radiolytic dissolution or assuming dissolution under reducing conditions or based on U solubility control have been tested. In order to put into perspective the importance of dissolution rate, the simulations have also taken into account uncertainties associated with other parameters involved in the release of activity, such as the IRF and fuel inventory, as well as parameters characterizing the properties of the repository components, such as sorption coefficients and diffusion and advection rates.

SP1 and SP2 calculation results converge to the same conclusions. The IRF and fuel dissolution rates are important parameters in a performance assessment, since they influence the release and migration of activity through the repository components for near and far fields. However, the properties of the disposal components (notably sorption, diffusion and advective flows) also strongly influence the transfer of radionuclides to the repository outlets. Therefore, it was stressed in the different calculations that taking into account uncertainties associated with

the repository component properties in addition to those associated with the source term parameters lead to a wide dispersion of the results.

4 Future research needs

The MICADO Project has proven valuable for addressing all aspects of uncertainty in relation to modeling spent fuel behaviour in a repository. In addition, it has also provided a platform for discussion among most of the world's specialists in this field. As a result, throughout the project the results of relevant recently published and ongoing studies on spent fuel and radiolysis were discussed and, where appropriate, incorporated into the conceptual and physico-chemical models. The work in the project therefore permitted future research areas to be identified, as discussed below.

Instant release fraction

The instant release fraction dominates potential dose contributions from spent fuel in most PA over the first 10000 years. Certain key input data to PA like IRF values of iodine, chlorine, carbon, selenium are still largely unknown and are represented by bounding values that remain to be confirmed. Areas of particular importance for the evaluation of the IRF include:

- Improvements in the understanding of the distribution of fission gas releases (FGR) for reactor fuels are necessary in order to provide more realistic relationships between FGR and release of various fission products, in particular ^{129}I, ^{79}Se and ^{135}Cs. The present approach correlates 'typical' values of FGR with IRF measurements. What is more relevant is the true weighted average FGR for the reactor fuels in question, which can be calculated using validated FGR codes for the burn-up ranges in question. This approach has recently been used for Swedish and Swiss reactors to provide a secure basis for obtaining average FGR values for high burn-up fuels (SKB 2009), but should also be extended to other cases.
- Relationships between the available fission gas release data and sparingly available iodine release data are known for CANDU fuel but must still be further developed for LWR fuel. Data on ^{36}Cl and ^{14}C are also largely absent. IRF values of ^{129}I, ^{14}C and ^{36}Cl have not been updated due to the lack of data. The corresponding research is very expensive but since iodine is the principal dose contributing nuclide in many PA, results are expected to have a direct impact on the predicted repository performance and the associated uncertainties. This is a particularly relevant issue for disposal of high burn-up fuel, where there are only few data. High burnup fuel is becoming increasingly important in current European nuclear energy use.
- In order to take credit for long-term retention of fission products in grain boundaries, it is necessary to develop a robust and validated mechanical model of grain boundaries. These models will have to be developed and checked with independent experimental datasets. Grain boundary release may also be important under reducing conditions, as recent data (Vandenborre et al. 2009) show that dissolution of sintered ThO_2 occurs preferentially at grain boundaries.
- Bounding values for the IRF for MOX fuel have been determined based on the FGR from the matrix to the gap and into pores in the high burnup structure. These IRF values are so high that their application in safety assessment would suggest that MOX fuel would be only a negligible barrier to the release of nuclides. In contrast, the few IRF measurements made on MOX fuel indicate significantly lower releases. Further IRF

measurements are needed for MOX fuel, as well as an assessment of the long-term stability of the high burnup zones (see previous point). By developing a mechanical model for grain boundaries, one should be able to replace these conservative bounding values with more realistic estimates for the quantitative assessment of the IRF for MOX fuel.

Fuel matrix dissolution

Previous EC projects have collected considerable data on spent UO_2 fuel matrix behavior and detailed models are available on the effect of radiolysis and environmental parameters such as pH, O_2, HCO_3, H_2O_2 and hydrogen. Nonetheless, a number of uncertainties remain:

- A physico-chemical mechanism for the observed suppression of radiolytic oxidation of alpha-doped UO_2 in the presence of hydrogen has been proposed but it remains to be confirmed. It is clear that the effect is principally a result of surface-mediated reactions, as the solution impacts on the radiolytic yield of oxidants are insufficient to account for the dramatic effects. Further work should be done to understand the mechanism.
- The beneficial effect of H2 in reducing the potentially oxidizing effect of alpha radiolysis is known only for relatively simple solutions that are not representative of repository groundwaters. It should be validated also for more realistic field conditions (presence of other phases, presence of various groundwater species…)
- The mechanistic understanding of the dose threshold and probably of the hydrogen effect is connected to the radiolytic yield of hydrogen peroxide for alpha particles emitted from UO2 surfaces. Fundamental studies on interfacial radiolysis are practically missing in Europe and applied research related to alpha-doped fuel is only about a decade old.
- Differences in the specific surface area of UO_2 and spent fuel need to be understood better to reduce uncertainties in drawing conclusions from UO_2 behavior for assessing spent fuel performance. In particular it has been observed that surface area increases with the extent of corrosion (for oxidizing conditions), whereas leaching rate decrease with time. This apparent contradiction must be fully understood, if one wants to use data from unirradiated UO_2 to quantitatively predict spent fuel behavior.
- Data on MOX fuel are still rather limited and allow no realistic prediction of fuel performance in a repository under hydrogen-saturated iron-rich conditions.
- The long-term behavior of the fuel matrix below the alpha dose threshold is considered being controlled either by solubility constraints or by slow kinetic rate laws. Consequences for PA are quite different for the both cases. Only a dedicated experimental approach on slow exchange processes close to equilibrium can resolve this uncertainty.

Spent fuel behavior under unsaturated conditions

Depending on repository concept, the time for saturation may take many thousands of years and the fuel may remain in contact with a hydrogen saturated vapor phase for long periods of time. In the NF-PRO project first experiments on vapor phase hydration of spent fuel have been dominated by condensed water

- Hydration tests shall be continued focusing on the effect of vapor pressure, temperature gradients and geometrical constraints
- Models shall be developed describing fuel behavior under non-saturated conditions.

- It is not clear whether the results of this study will have any direct influence on PA but the still missing data reduces the confidence in system understanding.

Effect of near field materials on fuel matrix dissolution

First data on clay/spent fuel interface interactions and batch iron/spent fuel systems have been generated in the NF-PRO and previous EC projects. Compared with the large database on simple spent fuel/UO2 /water systems the obtained data are still scarce and not yet conclusive.

- More data with well defined spent fuel/materials interfaces (spent fuel or homologues + either bentonite, clay, iron or cement) must be gathered allowing for realistic flow conditions.
- While models exist describing spent fuel behavior in different groundwaters, models describing the interaction of near field materials with spent fuel behavior have still to be developed. The possibility that the interactions may have non-linear impacts on the dissolution rate should be resolved.
- Key emphases are on studying coupling effects and improving overall systems understanding.

5 *References*

1. L. Johnson, C. Poinssot, C. Ferry, P. Lovera, Estimation of the Instant Release Fraction of UO2 and MOX fuel at t=0. Nagra Technical Report O4-08 (2004)

2. B. Hanson, R. Stout, Reexamining the dissolution of spent fuel: a comparison of different methods for calculating rates, Materials Research Society, Mat. Res. Soc. Symp. Proc. 824, 89-94 (2004)

3. W. Gray, R. Wilson, Spent fuel dissolution studies FY 1991 to 1994, PNNL 10540 Pacific Northwest Laboratory, Richland, WA, USA (1995)

4. R. Forsyth, The SKB Spent Fuel Corrosion Programme. An evaluation of results from the experimental programme performed in the Studsvik Hot Cell Laboratory, SKB 97-25, Stockholm (1997)

5. S. Röllin, K. Spahiu, U-B. Eklund, Determination of dissolution rates of spent fuel in carbonate solutions under different redox conditions with a flow-through experiment, *J. Nucl. Mater.* **297** pp. 231-243 (2001).

6. R. Forsyth, Spent nuclear fuel. A review of properties of possible relevance to corrosion processes, SKB 95-23, Stockholm (1995)

7. E.Iglesias, J. Quinones, Applied surface science,254 (2005) 6890-6896

8. Ollila K. 2008. Dissolution of unirradiated UO2 and UO2 doped with 233U in low- and highionic-strength NaCl under anoxic and reducing conditions. Final activity report for VTT (WP1.5), NF-PRO Deliverable 1.5.21.

9. Stroes-Gascoyne, S., Johnson, L. H., Tait, J. C., McConnell, J. L., Porth, R. J., Leaching of used CANDU fuel: Results from a 19-year leach test under oxidizing conditions, Materials Research Society, Mat. Res. Soc. Symp. Proc. 465, 551-558 (1997)

10. K.H. Schmidt, Measurement of the activation energy for the reaction of the hydroxyl radical with hydrogen in aqueous solution, J. Phys. Chem, **81** 1257-1263 (1977).

11. K. Spahiu, D. Cui, M. Lundström, The fate of radiolytic oxidants during spent fuel leaching in the presence of dissolved near field hydrogen, Radiochimica Acta, **92** 625-629 (2004).

12. P. Carbol, J. Cobos-Sabate, J-P. Glatz, B. Grambow, B. Kienzler, A. Loida, A. Martinez Esparza Valiente, V. Metz, J. Quiñones, C. Ronchi, V. Rondinella, K. Spahiu, D. H. Wegen, T. Wiss, The effect of dissolved hydrogen on the dissolution of ^{233}U doped UO_2(s), high burnup spent fuel andMOX fuel, SKB Technical Report TR-05-09, Stockholm(2005), 139 p.

13. E. Ekeroth, M. Granfors, D. Schild, K. Spahiu, The effect of temperature and fuel surface area on spent fuel dissolution kinetics under H2 atmosphere, Proceedings Migration 07, Munich (2007).

14. P.Carbol, P. Fors, S. Van Winckel , K. Spahiu K, Corrosion of irradiated MOX fuel in presence of dissolved H2, J. Nucl. Mater, **392**, pp. 45-54 (2009).

15. P. Fors, P. Carbol, S. Van Winkel and K. Spahiu, Corrosion of high burn-up structured UO2 fuel in the presence of dissolved H2, J. Nucl. Mater. **394**, pp.1-8 (2009).

16. D. Rai, A. R. Felmy, and J. L. Ryan, Uranium(IV) hydrolysis constants and solubility product of UO2.xH2O(am), Inorg. Chem. **29** 260-264 (1990).

17. A.Loida, V. Metz, B. Kienzler, Alteration behavior of high burnup spent fuel in salt brine under hydrogen overpressure and in presence of bromide, Mat. Res. Soc. Symp. Series, **985** 15-20 (2007).

18. V. Metz, E. Bohnert, M. Kelm, D. Schild, J. Reinhardt, B. Kienzler and M. Buchmeiser, γ-radiolysis of NaCl brine in presence of UO2(s): effects of hydrogen and bromide, Mat. Res. Soc. Symp. Series, **985** 33-40 (2007).

19. D**.** Zehavi, J. Rabani, J. Phys. Chem. 76 (1972) 312-319.

20. B. Pastina, and J. A. LaVerne, Effect of molecular hydrogen on hydrogen peroxide in water radiolysis, J. Phys. Chem. A **105** 9316-9322 (2001).

21. D. Cui, E. Ekeroth, P. Fors, K. Spahiu, Surface mediated processes in the interaction of spent fuel or α-doped UO2 with H2, Mat. Res. Soc. Symp. Proc. Vol. **1104**, pp. 87-99.

22. T**.** Eriksen, M. Jonsson, The effect of hydrogen on dissolution of spent fuel in 0.01 M NaHCO3 solution, SKB Techical Report TR-07-06, Stockholm (2007), 19 p.

23. E. Cera, J. Bruno, L. Duro, T. Eriksen, Experimental determination and chemical modelling of radiolytic processes at the spent fuel/water interface. Long contact time experiments, SKB TR-06-07, Stockholm 2006.

24. T. Eriksen, M. Jonsson, J. Merino, Modelling time resolved and long contact time dissolution studies of spent nuclear fuel in 10 mM carbonate solution-A comparison between two models and experimental data, J. Nucl. Mater., **375** 331-339 (2008).

25. K. Spahiu, L. Werme, U-B. Eklund, The influence of near field hydrogen on actinide solubilities and spent fuel leaching, Radiochim Acta, **88** 507-511 (2000).

26. Y. Albinsson, A Jensen, V. Oversby, L. Werme, Leaching of spent fuel under anaerobic and reducing conditions, Mat. Res. Soc. Symp., **757** 407-413 (2003).

27. K. Ollila, Y. Albinsson, V. Oversby, M. Cowper, Dissolution rates of unirradiated UO2, UO2 doped with 233U, and spent fuel under normal atmospheric conditions and under reducing conditions using an isotope dilution method, SKB Technical Report TR-03-13, (2003).

28. K. Spahiu, U-B Eklund, D. Cui, M. Lundström, The influence of near field redox conditions on spent fuel leaching, Mat. Res. Soc. Symp., **713** 633-638 (2002).

29. A. Loida, B. Grambow, H. Geckeis, Spent fuel corrosion behavior in salt solution in the presence of hydrogen overpressure Proceedings ICEM 01, Bruges, Belgium, (2001).

30. A. Loida, V. Metz, B. Kienzler, and H. Geckeis, Radionuclide release from high burnup spent fuel during corrosion in salt brine in the presence of hydrogen overpressure, J. Nucl. Mat. **346** (2005) 24-31.

31. M. Jonsson, F. Nielsen, E. Ekeroth, T. Eriksen, Modeling of the effects of radiolysis on UO_2 dissolution employing recent experimental data, Mat. Res. Soc. Symp., **807** 385-390 (2003)**.**

32. L. Liu and I. Neretnieks, The effect of hydrogen on the oxidative dissolution of spent fuel, Nuclear Technology, **138** 69-77 (2002)**.**

33. B.Grambow, A. Loida, P. Dressler, H. Geckeis, J.Gago, I. Casas, J. de Pablo, J. Gimenez, M.E. Torrero, Long-term safety of radioactive waste disposal: Chemical reaction of fabricated and high burnup spent fuel with saline brines, FZKA Report **5702**, Forschungszentrum Karlsruhe**, (**1996).

34. B.Grambow, A. Loida, A. Martinez-Esparza, P. Diaz-Arocas, J. de Pablo, J.-L. Paul, G.Marx, J.-P.Glatz, K.Lemmens, K. Ollila, H. Christensen, Source term for performance assessment of spent fuel as a waste form, European Commission, EUR **19140** EN, (2000).

35. J. Farrel, W. Bostick, R. Jarabek, N. Fiedor, Uranium removal from ground water using zero valent iron media, Ground Water **37**(4), 618 (1999).

36. D. Cui, K. Spahiu, The reduction of U(VI) on corroded iron under anoxic groundwater conditions, Radiochim. Acta, **90** 1-6 (2002).

37. F. King, M. J. Quinn and H. H. Miller, The effect of hydrogen and gamma radiation on the oxidation of UO2 in 0.1 mol·dm-3 NaCl solution, SKB Technical Report TR-99-27 (1999).

38. D. W. Shoesmith, The role of dissolved hydrogen on the corrosion/dissolution of spent nuclear fuel, NWMO Technical Report TR-2008-19, Toronto (2008).

39. S. Sunder, G. D. Boyer, N. H. Miller, XPS studies of UO2 oxidation by alpha radiolysis of water at 100 ºC, J. Nucl. Mater. **175** 163-169 (1990).

40. M. E. Broczkowski, J. Goldik, B. Santos, J. Noel and D. Shoesmith, Corrosion of nuclear fuel inside a failed copper nuclear waste container Mat. Res. Soc. Symp. Proc. **985** 3-14 (2006).

41. M. E. Broczkowski, J. J. Noel and D. W. Shoesmith, The inhibiting effects of hydrogen on the corrosion of uranium dioxide under nuclear waste disposal conditions, J. Nucl. Mat. **346** 16-23 (2005).

42. M. E. Broczkowski, J. Noel and D. Shoesmith, The influence of dissolved hydrogen on the surface composition of doped uranium dioxide under aqueous corrosion conditions, J. Electroanal. Chem. **602** pp. 8-16 (2007).

43. M. Trummer, S Nilsson, M. Jonsson, On the effects of fission product noble metal inclusions on the kinetics of radiation induced dissolution of spent nuclear fuel, J. Nucl. Mater. **378** pp. 55-59, 2008.

44. M. Jonsson, F. Nielsen, O. Roth, E. Ekeroth, S. Nilsson and M. Hossain, Radiation induced spent nuclear fuel dissolution under deep repository conditions Environ. Sci. Technol. **41** 7087-7093 (2007).

45. S. Nilsson, M. Jonsson, On the catalytic effect of UO2(s) and Pd(s) on the reaction between H_2O_2 and H_2 in aqueous solution, J. Nucl. Mat., **372** 160-163 (2008).

46. D. Cui, J. Low, C. J. Sjöstedt, K. Spahiu, On Mo-Ru-Tc-Pd-Rh alloy particles extracted from spent fuel and their leaching behavior under repository conditions, Radiochim. Acta, **92** 551-555 (2004).

47. B. Muzeau, Ph. D. Thesis, University Paris XI, (Orsay 2007), 274p.

48. V. Rondinella, J. Cobos and T. Wiss, Leaching Behaviour of Low-Activity Alpha-Doped UO2, Mat. Res. Soc. Symp. Proc., **824** 167-174 (2004).

49. C. Jegou, B. Muzeau, V. Broudic, A. Poulesquen, D. Roudil, F. Jorion and C. Corbel, Effect of alpha irradiation on UO2 surface reactivity in aqueous media, Radiochim. Acta **93**, 35–42 (2005).

50. B. Muzeau, C. Jégou, F. Delaunay, V. Broudic, A. Brevet, H. Catalette, E. Simoni, Radiolytic oxidation of UO2 pellets doped with alpha emitters (238/239Pu), J. All. Comp. 467, pp. 578-589.

51. P. Carbol, P. Fors, T. Gouder, K. Spahiu, Hydrogen suppresses nuclear waste corrosion, Geochim. Cosmochim. Acta, **73**, 4366-4375, (2009).

52. A.Ö. Jensen, P. Fors, G. Skarnemark, Y. Albinsson, Oxygen production from alpha radiolysis in homogeneous H2 containing solutions, Deliv. 1.5.3, EU-NF-PRO (2006).

53. K.Spahiu, Deliverable 1.5.20, EU-NF-PRO (2006).

54. B. G. Santos, J.J. Noël, D.W. Shoesmith, The influence of Ca ions in the development of acidity in corrosión product deposits on SIMFUEL, UO_2, J. Nucl. Mat.**350**, pp.320-331(2006).

55. D. Cui, J. Devoy, K. Spahiu, The surface precipitation during UO2 leaching process, Mat. Res. Soc. Symp. Proc. **757** 359-364 (2003).

56. B. G. Santos, J.J. Noël, D.W. Shoesmith, The influence of silicate in the development of acidity in corrosión product deposits on SIMFUEL(UO_2), Corr. Sci.**48** pp.3852-3868(2006).

57. K.A. Cliffe and M. Kelly, COMP23 v1.2.2 Users manual, SKB R-04-64, Stockholm 2004.

58. A. Lasaga, Kinetic theory in the earth sciences, Princeton University Press, Princeton, New Jersey, 1998.

59. (a) Röllin S., Spahiu K., Eklund U.-B. *J. Nucl. Mater.* (2001), 297, 231-243. (b) Spahiu K., Eklund U.-B., Cui D., Lundström M. *Scientific Basis for Nuclear Waste Management XXV* (2002), 713, 633-638, Mat. Res. Soc. Symp. Series. (c) Spahiu K., Cui D., Lundström M. *Radiochim. Acta*, (2004), 92, 625-629. (d) Carbol P., Cobos-Sabate J., Glatz J.-P., Ronchi C., Rondinella V., Wegen D. H., Wiss T., Loida A., Metz V., Kienzler B., Spahiu K., Grambow B., Quiñones J., Martínez-Esparza A. SKB Technical Report, (2005), TR-05-09.

60. Bruno J., Merino J., Tamayo A., Ferry C., Quiñones J., Iglesias E., Rodriguez Villagra N., Nieto J. M., Martínez-Esparza A., Loida A., Metz V., Jonsson M., Ekeroth E., Grambow B. (2009). Deliverable 3.1: Application of models to selected datasets. MICADO project (priority nº NUWASTE-2005/6-3.2.1.1-2), Work Package 3. European Commission. 6th Framework Programme. EURATOM Specific Programme for Research and Training on Nuclear Energy.

61. Pastina B., Laverne J. Effect of Molecular Hydrogen on Hydrogen Peroxide in Water Radiolysis. *J. Phys. Chem. A*, (2001), 105, 9316-9322.

62. Trummer M., and Jonsson M., to be published.

63. (a) Broczkowski M. E., Noël J. J., Shoesmith D. W. J. Nucl. Mater. 346 (2005) 16-23, (b) Trummer M., Nilsson S., Jonsson M. *J. Nucl. Mater.* 378 (2008) 55-59, (c) Eriksen T. E., Jonsson M., Merino J. *J. Nucl. Mater*. 375 (2008) 331-339

64. D.H. Wegen, P.D.W. Bottomley, J.-P. Glatz, J. Giménez, A.D. Stalios, F. Montigny, G. Pagliosa, D. Pellottiero, R. Cremer, K. Römer, E. Teixeira, *Source term for performance assessment of spent fuel as a waste form, Final Report for the EU R&T Programme "Nuclear Fission Safety 1994-1998"*, Contract FI4W-CT95-0004, JRC-ITU-SCA-99/02, Karlsruhe, 1999

65. C.A. *Schiller*, *Introduction to Electrochemical Instrumentation*, pp. 361-505, in: Analytical Methods in *Corrosion* Science and Engineering, edited by P. Marcus, F. Mansfeld, CRC Press, Boca Raton, 2006

66. V.S. Bagotsky, Fundamentals of Electrochemistry, John Wiley & Sons, Hoboken, 2006

67. D.H. Wegen, P.D.W. Bottomley, M. Coquerelle, The construction of a micro-cell for electrochemical monitoring of spent fuel leaching, Proc. 189th Meeting of the Electrochemical Society, 5. - 10. May 1996, Los Angeles, USA
68. J. Römer, M.Plaschke, G.Beuchle, J.I. Kim, In situ investigation of U(IV)-oxide surface dissolution and remineralization by electrochemical AFM, J. Nucl. Mater. **322** (2003) 80–86
69. F.N. Skomurski, R.C. Ewing, A.L. Rohl, J.D. Gale, U. Becker, Quantum mechanical vs. empirical potential modelling of uranium dioxide (UO2) surfaces: (111), (110), and (100), Am. Mineral. 91 (2006) 1761-1772

70. H. He, R. K. Zhu, Z. Qin, P. Keech, Z. Ding, D. W. Shoesmith, Determination of Local Corrosion Kinetics on Hyper-Stoichiometric UO_{2+x} by Scanning Electrochemical Microscopy, J. Electrochem. Soc. **156** (2009) C87-C94

71. S. Salah, C. Cachoir, K. Lemmens and N. Maes, Static dissolution tests of □-doped UO_2 under repository relevant conditions: Influence of Boom Clay and a-activity on fuel dissolution rates, MRS Symp. Proc. Vol. 932 (2006), pp. 481-488

72. F.Puig, J.Dies, M.Sevilla, J.De Pablo, J.J.Pueyo, L.Miralles, A. Martinez-Esparza, Inner material candidates selection and evaluation for spanish high level radioactive waste canister, Paper 7178 in Proceedings of ICEM'07, Sep 2-6, 2007, Bruges (Brugge), Belgium

73. B. Grambow and E. Giffaut, Coupling of chemical processes in the near field, Mat.Res.Soc. Symp.Proc. Vol 932, 2006, pp 55-66

74. N. Maes et al., Uranium retention and migration behaviour in Boom Clay, NIROND-TR report 2007-10, 2004

75. Werme, L. O. , Johnson, L. H. ,Oversby, V. M, King, F., Spahiu, K., Grambow, B. , Shoesmith, D. W., Spent fuel performance under repository conditions: A model for use in SR-Can. SKB Technical Report TR 04-19, Stockholm (2004)

76. Casas et al. 1998

77. Janeczek et al. 1998

78. (a) Deditius A. P., Utsunomiya S., Ewing R. C. The chemical stability of coffinite, USiO4·nH2O; 0<n<2, associated with organic matter: A case study from Grants uranium region, New Mexico, USA. Chem. Geol. (2008), 251, 33-49. (b) Amme M., Wiss T., Thiele H., Boulet P., Lang H. Uranium secondary phase formation during anoxic hydrothermal leaching processes of UO_2 nuclear fuel. J. Nucl. Mat. (2005), 341, 209-223. (c) Bros R., Hidaka H., Kamei G., Ohnuki T. Mobilization and mechanisms of retardation in the Oklo natural reactor zone 2 (Gabon)-interferences from U, REE, Zr, Mo and Se isotopes. Appl. Geochem. (2003), 18,

1807-1824. (d) Jensen ,K. A.; Ewing, R. C. The Okélobondo natural fission reactor, southeast Gabon; Geology, mineralogy, and retardation of nuclear-reaction products. Geological Society of America Bulletin, (2001), 113(1), 32-62.

79. Janeczek J., Ewing R. C. Uraninite from Cigar Lake: Drill cores 220 and FH-18. Final Report of the AECL/SKB Cigar Lake Analog Study, (1994). (Cramer J.J., Smellie J.A.T. eds.). AECL Research, 93-103.

80. (a) Grenthe, I., Fuger, J., Konings, R.J.M., Lemire, R.J., Muller, A.B., Nguyen-Trung, C., Wanner, H. Chemical Thermodynamics 1; Chemical Thermodynamics of Uranium (1992), (Wanner H. and Forest I. eds.). NEA OECD, Elsevier. (b) Guillaumont, R., Fanghänel, J., Neck, V., Fuger, J., Palmer, D. A., Grenthe, I., Rand, M. H. Chemical Thermodynamics 5. Update on the Chemical Thermodynamics of Uranium, Neptunium, Plutonium, Americium and Technetium. (2003) NEA OECD, Elsevier.

81. Janaczek and Ewing 1992

82. Min, M., Fang, C., Fayek, M. Petrography and genetic history of coffinite and uraninite from the Liueryiqi granite-hosted uranium deposit, SE China. Ore Geology Reviews (2005), 26, 187-197.

83. Cramer and Smellie 1992

84. Smellie and Karlsson 1996

85. Ferry C., Grambow B., Jonsson M., Martinez-Esparza A., Mennecart T., Poulesquen A., Quinones J. (2008). Description of radionuclides source term models. Deliverable D1 of the MICADO project (priority nº NUWASTE-2005/6-3.2.1.1-2). European Commission. 6th Framework Programme.

86. Bruno J., Merino J., Tamayo A., Ferry C., Quiñones J., Iglesias E., Rodriguez Villagra N., Nieto J. M., Martínez-Esparza A., Loida A., Metz V., Jonsson M., Ekeroth E., Grambow B. (2009). Deliverable 3.1: Application of models to selected datasets. MICADO project (priority nº NUWASTE-2005/6-3.2.1.1-2), Work Package 3. European Commission. 6th Framework Programme. EURATOM Specific Programme for Research and Training on Nuclear Energy.

87. Poinssot C., Ferry C., Kelm M., Grambow B., Martínez A., Johnson L., Andriambololona Z., Bruno J., Cachoir C., Cavedon J.M., Christensen H., Corbel C., Jegou C., Lemmens K., Loida A., Lovera P., Miserque F., de Pablo J., Poulesquen A., Quiñones J., Rondinella V., Spahiu K., Wegen D.H. (2005). Final Report of the Spent Fuel Stability under Repository Conditions (SFS). European Commission. 5th Euratom Framework Program, contract nº FIKW-CT-2001-00192.

88. (a) Casas I., Giménez J., Martí V., Torrero M. E., de Pablo J. (1994). Kinetic studies of unirradiated UO_2 dissolution under oxidizing conditions in batch and flow experiments. Radiochimica Acta, 66-67(1). (b) Meca S., Martí V., de Pablo J.,

Giménez J., Casas I. (2008). UO_2 dissolution in the presence of hydrogen peroxide at pH>11. Radiochimica Acta, 96(9-11), 535-539. (c) Casas I., Borrell M., Sanchez L., de Pablo J., Gimenez J., Clarens F. (2008). Determination of UO_2(s) dissolution rates in a hydrogen peroxide medium as a function of pressure and temperature. Journal of Nuclear Materials, 375(1), 151-156.

89. (a) Bruno J., Casas I., Puigdomènech I. (1988). The kinetics of dissolution of UO_2(s) under reducing conditions. Radiochimica Acta, 44/45, 11-16. (b) Bruno J., Casas I., Puigdomènech I. (1991). The kinetics of dissolution of UO_2 under reducing conditions and the influence of an oxidized surface layer (UO_{2+x}): Application of a continuous flow-through reactor. Geochimica et Cosmochimica Acta, 55, 647-658.

90. Maynard J. B. (1983). Geochemistry of Sedimentary Ore Deposits. Springer-Verlag, New York.

91. Ollila, Kaija , Albinsson, Yngve, Oversby, Virginia, Cowper, Mark, Dissolution rates of unirradiated UO_2, UO_2 doped with ^{233}U, and spent fuel under normal atmospheric conditions and under reducing conditions using an isotope dilution method, SKB technical report TR 03-13, Stockholm (2003)

92. Bruno J., Merino J., Tamayo A., Ferry C., Quiñones J., Iglesias E., Rodriguez Villagra N., Nieto J. M., Martínez-Esparza A., Loida A., Metz V., Jonsson M., Ekeroth E., Grambow B. (2009). Deliverable 3.1: Application of models to selected datasets. MICADO project (priority nº NUWASTE-2005/6-3.2.1.1-2), Work Package 3. European Commission. 6th Framework Programme. EURATOM Specific Programme for Research and Training on Nuclear Energy.

93. Bruno J., Duro L., Tamayo A., Ferry C., Quiñones J., Iglesias E., Rodriguez Villagra N., Martínez-Esparza A., Loida A., Metz V., Jonsson M., Van Iseghem P., Marivoet J., Ekeroth E., Grambow B. (2009). Deliverable 3.2: Comparison of fitting strategies and uncertainty analyses. MICADO project (priority nº NUWASTE-2005/6-3.2.1.1-2), Work Package 3. European Commission. 6th Framework Programme. EURATOM Specific Programme for Research and Training on Nuclear Energy.

European Commission

EUR 24597 – MICADO – Model Uncertainty for the Mechanism of Dissolution of Spent Fuel in Nuclear Waste Repository

Luxembourg: Office for Official Publications of the European Communities

2010 — 64 pp. — format, e.g. 21.0 x 29.7 cm

ISBN 978-92-79-17652-4

doi 10.2777/25846

How to obtain EU publications

Publications for sale:

- via EU Bookshop (http://bookshop.europa.eu);
- from your bookseller by quoting the title, publisher and/or ISBN number;
- by contacting one of our sales agents directly. You can obtain their contact details on the Internet (http://bookshop.europa.eu) or by sending a fax to +352 2929-42758.

Free publications:

- via EU Bookshop (http://bookshop.europa.eu);
- at the European Commission's representations or delegations. You can obtain their contact details on the Internet (http://ec.europa.eu) or by sending a fax to +352 2929-427